8-2011

Evaluating the Capacity of a Proton Therapy Facility

Ridvan Gedik
University of Arkansas, Fayetteville

EVALUATING THE CAPACITY OF A PROTON THERAPY FACILITY

EVALUATING THE CAPACITY OF A PROTON THERAPY FACILITY

A thesis submitted in partial fulfillment
of the requirements for the degree of
Master of Science in Industrial Engineering

By

Ridvan Gedik
Middle East Technical University
Bachelor of Science in Industrial Engineering, 2009

August 2011
University of Arkansas

Abstract

A relatively new consideration in proton therapy planning is the requirement that the mix of patients treated satisfy desired percentages. Since it is very difficult to satisfy an integer number of patients in light of these requirements, deviations from patient mix preferences and their impacts on operational capabilities are of particular interest to healthcare planners. Therefore, we propose a bicriteria mathematical programming model that determines an outpatient schedule maximizing the number of fractions and minimizing the deviations from the patient mix ratios over the planning horizon. The tradeoffs between the two objectives are identified through analysis of efficient frontiers. Our models are applicable to healthcare treatment facilities throughout the United States, but are motivated by collaboration with the University of Florida Proton Therapy Institute (UFPTI) in Jacksonville, Florida.

This thesis is approved for recommendation
to the Graduate Council

Thesis Director:

Prof. Chase Rainwater

Thesis Committee:

Prof. Edwin Romeijn

Prof. Ronald Rardin

Thesis Duplication Release

I hereby authorize the University of Arkansas Libraries to duplicate this Thesis when needed for research and/or scholarship.

Agreed ____________________________________

Ridvan Gedik

Refused ____________________________________

Ridvan Gedik

Acknowledgements

I would like first to express my sincere gratitude to Dr. Chase Rainwater, may advisor, for his endless encouragement and support. It is one of the greatest privilege in my life to work with such a great mentor and outstanding faculty. I am also grateful to my committee members, Dr. Edwin Romeijn and Dr. Ronald Rardin for their invaluable feedbacks and guidance throughout this thesis.

Also, special thanks to the faculty and staff at the INEG department of University of Arkansas for their commitment and care to its students.

My sincere thanks also go to each member of "çiğ̃köftEM" and my graduate student colleagues for their kind friendships.

Finally, special thanks go to my siblings for their continuous and unconditional supports during all phases of my life. Most importantly, I would like to thank to my beloved parents, Dursun and Şerife Gedik, for their love and sacrifices. This work is dedicated to my family.

Contents

List of Figures

List of Tables

1 Introduction

Proton therapy is a relatively new and fast growing form of radiation therapy for cancer patients. To date, more than 40,000 people have been treated at 25 proton therapy centers around the world [1]. Due to the effectiveness and limited availability of proton therapy, the demand for this form of treatment is extremely high in relationship to the available capacity. Moreover, it is an expensive treatment procedure to deliver. According to the study by Goitein et al. [2], the cost-per-fraction in proton therapy is more than two times the cost-per-fraction of X-ray therapy. A portion of these high costs can be attributed to the small number of proton therapy facilities in the country (9 in use and 3 are under construction). An equally important driver of cost is the meticulous process that must be followed to successfully deliver this form of treatment. In fact, in radiation therapy, a treatment protocol consists not only of a prescribed total delivered dose to so-called targets, but must also specify treatment times, sequences, and frequencies (fractionation schedule). It is known that dose fractionation contributes to the preservation of healthy tissue throughout the treatment (see, e.g., Yamada et al. [3]). However, a shorter fractionation schedule provides a more economical use of the radiation therapy facilities while still improving, albeit marginally, a patient's quality of life (see, e.g., Shelley et al. [4]). Because of these important tradeoffs, efficient patient scheduling is a growing area of interest to healthcare professionals.

Over the past 50 years, a large amount of health care scheduling literature has been developed. In most of the studies, operation/emergency room, nurse and physician scheduling problems are considered. Cardoen et al. [5] proposed a detailed review on operating room planning and scheduling. In this study, previous work can be characterized in terms of problem structures and technical features. One class of problems is based on the classification of patients in two major classes based on individual patient characteristics; elective (operation is planned in advance) and non-elective (unexpected operation). The former includes inpatient (stay overnight) and outpatient (enter and leave on same day) categories as well. In most of the studies (e.g., Bowers and Mould [6], Cayirli et al. [7], and Pham and Klinkert [8]), elective cases are considered in order to reduce potential uncertainties patient attributes (i.e., patient type, financial gain, resource allocation per patient, etc.). In other studies, treatment time for an outpatient is assumed to be constant for the sake of simplicity (see, e.g., Conforti et al. [9]).

Most commonly, patient scheduling problems seek to maximize the number of scheduled patients (see, e.g., Conforti et al.[10], Ballard and Kuhl [11], and Cardoen and Demeulemeester [12]) subject to case-specific constraints combined with prescribed treatment plans. Minimizing the waiting times of patients is also considered as an objective in a subset of works (see, e.g., Chaabane et al. [13] and Kaandorp and Koole [14]). Of course, these two objectives are complementary to each other. Under appropriate assumptions, we may use Little's Law to conclude that the average number of patients in the system is equal to average cycle time (treatment time and waiting time) multiplied by the average throughput (see Cardoen et al. [5]). Therefore, ultimately, reduced waiting times for the patients results in shorter workdays for doctors and an increased number of treated patients [15].

Conforti et al. [10] proposed an integer linear optimization program with the objective to maximize the number of new scheduled patients in a radiation therapy clinic. According to the pathological conditions, weights are assigned to patients in order to identify different patient groups. Patients are scheduled from two different lists; a waiting list refers to patients waiting to be scheduled and a booked list contains names of those patients already scheduled for the upcoming planning period (see Conforti et al. [9] as well). Both lists are dynamic, therefore patients scheduled for a planning period may be replaced with individuals from either list. For instance, a patient from the waiting list with an urgent condition can be rescheduled and added to the booked list during a planning period. Even though the decisions are based on a weekly horizon, utilization of linear accelerators are increased by rescheduling patients dynamically.

Another related study to our work was conducted by Mulholland et al. [16]. They proposed a linear program to determine the optimal mix of surgical procedures. They analyzed the effects of changes in these procedures on financial outcomes. Even though no more than 15% deviation in procedure mix is allowed, substantial financial gains (i.e. 16.1% increases in hospital total margin) are obtained due to small changes in procedure volume without any capacity investments. These desirable findings motivate further investigation into sophisticated models for efficient patient planning in the proton therapy healthcare environment.

Although our work and other patient scheduling problems share common properties (treatment continuity, capacity, staff/physician requirements etc.), the model in this study differs by aiming to accommodate patients from different categories without assigning them any priority weights related urgency level of disease. Instead, categories represent the different patient types. Each one of these types has different treatment time and number of fractions to be delivered. Moreover, similar to the case in [16], there is a restriction on each patient category that forces us to have a target value in terms of number of fractions for a patient category over the planning period.

Since it is very difficult to satisfy an integer number of patients in light of these requirements, deviations from patient mix preferences and their impacts on operational capabilities are of particular interest to healthcare planners. Therefore, we propose a bicriteria mathematical programming model that determines an outpatient schedule maximizing the number of fractions and minimizing the deviations from the patient mix ratios over the planning horizon. The tradeoffs between the two objectives are identified through analysis of efficient frontiers. Our models are applicable to healthcare treatment facilities throughout the United States, but are motivated by collaboration with the University of Florida Proton Therapy Institute (UFPTI) in Jacksonville, Florida.

The remainder of the study is organized as follows. Section 2 introduces the problem components in light of proton therapy scheduling problem of interest. Section 2.1 presents an integer linear program with the fundamental constraints considered by the medical decision to solve the proton therapy patient scheduling problem. Then, Section 2.2 specifies the various operational restrictions that may be required in scheduling different types of patients. A bicriteria optimization model is introduced in Section 2.3. Section 3 discusses the noninferior set estimation (NISE) method used to investigate the tradeoffs between patient fractions treated and the deviation from the desired patient mix. Section 4 demonstrates the results obtained by implementing the NISE algorithm for each operational restriction and a sensitivity analysis on model parameters. Finally, Section 5 provides a summary of the results and suggestions for future work.

2 Problem Description

Due to rising interest in proton therapy, healthcare planners are looking forward to increasing the utilization of the resources in proton therapy facilities in order to satisfy the growing demand for this technology. Decision makers must also take into account numerous other operational restrictions and their possible impacts on the facility capacity. Hence, the objective of this study is to provide efficient capacity planning for a proton therapy facility and to investigate the impact of various operational limitations, such as: (i)strategic patient mix ratios, (ii) physician availability, (iii) operating hours, (iv) number of available treatment gantries, (v) gantry specialization and (vi) gantry switching. Strategic patient mix ratios for patient categories is a relatively new consideration in proton therapy planning. It implies that the mix of patients treated in a planning period must satisfy the targeted percentages specified by managers. Further discussions about patient mix constraints, as well as other operational restrictions, are given throughout this section. In order to represent the impacts of these restrictions and perform capacity analysis over a physician-specified planning period, we propose an integer linear programming model in Section 2.1.

In the healthcare environment, uncertainty is one of the major obstacles encountered in scheduling problems. Appointment cancellations (no-show) are the most common sources of uncertainty in patient scheduling problems. However, the issue of rescheduling and treatment session cancellations require less consideration in this study than in other healthcare applications. Since there is always a huge demand for this therapy, the replacement of cancelled patients with the new patients in the waiting lists can be performed instantaneously without any waste in resources. This greatly reduces the uncertainty associated with scheduling patients to deliver treatments within a planning period. As a result, daily rostering and no-show are not considered in this study.

Cardoen et al. [5] characterized previous works conducted in health care scheduling according to specific problem structures and problem elements. Based on these criterion, patients in our study are classified as elective outpatient patients. This implies that even though consecutive daily appointments are required for proton therapy, patients do not typically stay at the hospital overnight.

We begin with an introduction of the notation used throughout the remainder of the document and then proceed to present what we will refer to as the *base model* of this study. The restrictions associated with varying operational issues and patient categories are also presented.

- **Sets**:

  T: set of days in planning horizon

  G: set of gantries

  K: set of patient categories

  K^a: set of patient categories needing anesthesia for treatment

K^2: set of categories for patients needing twice-a-day fractions

T_{NA}: set of non authorized days to start new patients

T_A: set of authorized days to start new patients

- **Parameters:**

C_{tg}: time available for treatment on gantry g on day t

n_k: number of consecutive treatment days for patients in category k

f_k: number of fractions required on each day of the treatment by a patient in category k

c_k: duration of a fraction on each day of the treatment by a patient in category k

$\bar{c}_k$: additional duration needed for the first fraction on the first treatment day for patients in category k

d_k: desired fraction of patients in category k treated over the planning horizon

w_k: total duration required for each patient from category k, $w_k = f_k n_k$

A_g: anesthesia availability per day on gantry g

τ: minimal time between two fractions (in minutes)

η_g: Available prime hours on authorized days to treat new patients

- **Decision variables:**

x_{tkg} : the number of new patients in category k that start their treatment on day t on gantry g

y_{tkg} : the number of patients in category k that receive treatment on day t on gantry g

2.1 Base Model

The so-called base model introduced in this section incorporates the three fundamental restrictions placed on a medical decision maker in a proton therapy treatment facility: (i) gantry capacity limitations, (ii) patient continuity requirements and (iii) patient mix specifications. Since we are considering a strategic capacity analysis, we prevent both end of study effects and the need for an excessively long planning horizon by assuming that the facility is operating in steady-state. Hence, we consider the planning period to be cyclic with a period length of T days.

$$\text{maximize} \sum_{t \in T} \sum_{k \in K} \sum_{g \in G} f_k y_{tkg}$$

subject to (B)

$$\sum_{n=1}^{n_k} x_{[t-n+1],kg} = y_{tkg} \qquad t \in T;\ k \in K\ g \in G \qquad (1)$$

$$\sum_{k \in K} \bar{c}_k x_{tkg} + \sum_{k \in K} c_k f_k y_{tkg} \leq C_{tg} \qquad t \in T;\ g \in G \qquad (2)$$

$$d_k \sum_{t \in T} \sum_{k' \in K} \sum_{g \in G} x_{tk'g} = \sum_{t \in T} \sum_{g \in G} x_{tkg} \qquad k \in K \qquad (3)$$

$$x_{tkg}, y_{tkg} \in \mathbb{Z} \qquad t \in T;\ k \in K;\ g \in G \qquad (4)$$

The objective function of problem (B) maximizes the total number of fractions treated over the planning cycle. Note that treatment continuity constraints (1) require that patients must be treated in the same gantry throughout their treatment plan. These constraints can be rewritten to allow for patients to switch gantries throughout the the planning horizon, if the decision maker is afforded this flexibility. This alternative representation of treatment continuity, which refer to as *allowable gantry switching*, is given in (5) as follows.

$$\sum_{g=1}^{G}\sum_{n=1}^{n_k} x_{[t-n+1],kg} = \sum_{g=1}^{G} y_{tkg} \qquad t \in T;\ k \in K. \tag{5}$$

Both constraints (1) and (5) enforce the appropriate relationship between two decision variables our problem; number of fractions and the number of patients. Each guarantees that fractions are delivered over a number of consecutive (week)days. Therefore, if the treatment of a patient in category k starts on day t, the following treatment days for this patient will be $t+1, \ldots, t+n_k-1$ for each k and t. Constraints (2) ensure that the limited operational capacity is enforced on each treatment day t and on each gantry g. Constraint set (3) specifies the desired patient mix ratios among the different categories in such a way that number of patients treated from category k over the total number of patients received treatments from all categories in a planning period must be equal to targeted percentages d_k.

2.2 Side Constraints

There are operational side constrains briefly listed in the problem description that impact the number of fractions to be treated over the specified horizon. In this section, we mention the limitations caused by these restrictions and give the corresponding mathematical representations in Sections 2.2.1 - 2.2.5.

2.2.1 Anesthesia Patients

Some patients need the surveillance of anesthesia teams while they are receiving their treatments. Constraints (6) assure that the treatment durations for these patients can not exceed the daily availability of anesthesia teams in each gantry on day t.

$$\sum_{k \in K^a} (\bar{c}_k x_{tkg} + c_k f_k y_{tkg}) \leq A_g \qquad t \in T;\ g \in G \tag{6}$$

2.2.2 BID Patients

Often, a subset of patients are required to receive two treatments on the same day. These patients are referred to as BID (*Bis In Die*, twice daily) patients and must be treated in the same order, on the same gantry and on a particular day. Hence, constraints (7) make sure that the second set of fractions for these patients starts at least $\tau + \max_{k \in K^2} c_k$ time units after the start of the day.

$$\sum_{k \in K^2} (\bar{c}_k x_{tkg} + c_k y_{tkg}) \leq C_{tg} - \tau - \max_{k \in K^2} c_k \qquad t \in T;\ g \in G \tag{7}$$

2.2.3 Gantry Specialization

Managers may want to specialize one or more gantries for the patients from specified categories in order to increase the service level. Therefore, if the patient categories in the set K_g ($g \in G$) are specialized to be treated in gantry g, then the following constraints should be enforced.

$$y_{tkg} = 0 \qquad t \in T;\ g \in G;\ k \in K \backslash K_g. \tag{8}$$

2.2.4 Prime Hours

Due to limited physicians' schedule, managers might need to restrict accepting new patients on specific days and deliver fractions in their physicians' presence. Consequently, constraint set (9) ensures that new patients can only start their treatment on authorized days (T_A) during so called prime hours (η_g) in each gantry.

$$\sum_{k \in K} (\bar{c}_k + c_k) x_{tkg} \leq \eta_g \qquad t \in T_A;\ g \in G \tag{9}$$

$$x_{tkg} = 0 \qquad t \in T_{NA};\ g \in G;\ k \in K \tag{10}$$

Also, constraints (10) prohibits starting new patient treatments on non authorized days (T_{NA}).

2.2.5 Capacity Exchange

From a personnel planning perspective, any consideration of overtime can be costly. Therefore, decision makers must understand the operational benefits made possible by manipulating the resource availability schedule. To model this change in case of prime hours restriction, we introduce a new decision variable δ_{tg} to represent the capacity exchange among gantries on authorized days ($t \in T_A$). Hence, constraints (2) is replaced by constraints (11) to include the flexibility gained by reallocating capacity. Constraints (12) ensure that excess capacity spent on gantry g is taken from other gantries on each authorized day $t \in T_A$. That is, the net change in total capacity used for a fixed day must be zero. Constraints (13) ensure that the maximum capacity taken from a gantry g on day t can not exceed n_g as well as extra time spent in a gantry can not exceed the leftover time $(C_{tg} - \eta_g)$ in a day. Finally, constraints (14) assure that capacity exchange can not be performed during non authorized days among gantries.

$$\sum_{k \in K} (\bar{c}_k + c_k) x_{tkg} \leq \eta_g + \delta_{tg} \qquad t \in T_A;\ g \in G \tag{11}$$

$$\sum_{g \in G} \delta_{tg} = 0 \qquad t \in T_A \tag{12}$$

$$-\eta_g \leq \delta_{tg} \leq C_{tg} - \eta_g \qquad t \in T_A;\ g \in G \tag{13}$$

$$\delta_{tg} = 0 \qquad t \in T_{NA};\ g \in G \tag{14}$$

$$\delta_{tkg} \quad urs \qquad t \in T;\ k \in K;\ g \in G \tag{15}$$

Alternatively, this relationship can be established by relaxing constraints (16) to allow for capacity exchange between gantries over the entire planning horizon among the authorized days..

$$\sum_{t \in T_A} \sum_{g \in G} \delta_{tg} = 0 \tag{16}$$

2.3 Bicriteria Optimization

Our initial investigation found that the patient mix constraints, in light of the integrality restrictions, result in a problem that becomes computationally intractable when solved using a black box optimization solver. Unfortunately, relaxing the integrality constraints is likely to lead to non-insightful solutions due to the large number of patient categories and relatively small number of patients on a given day. Therefore, we choose to pursue the following bicriteria optimization problem. This approach allows us evaluate the deviation from the desired patient mix ratios versus the total fractions treated. This evaluation will be aided by the construction of Pareto efficient frontiers for the following problem.

$$\text{maximize} \quad \left\{ \sum_{t=1}^{T} \sum_{k=1}^{K} \sum_{g=1}^{G} f_k y_{tkg}, - \sum_{k=1}^{K} u_k \right\}$$

subject to (M)

$$\sum_{n=1}^{n_k} x_{[t-n+1],kg} = y_{tkg} \qquad t \in T;\ k \in K$$

$$\sum_{k=1}^{K} \bar{c}_k x_{tkg} + \sum_{k=1}^{K} c_k f_k y_{tkg} \leq C_{tg} \qquad t \in T;\ g \in G$$

$$\sum_{t=1}^{T} \sum_{g=1}^{G} x_{tkg} \geq d_k \sum_{t=1}^{T} \sum_{k'=1}^{K} \sum_{g=1}^{G} x_{tk'g} - u_k \qquad k \in K \tag{17}$$

$$\sum_{t=1}^{T} \sum_{g=1}^{G} x_{tkg} \leq d_k \sum_{t=1}^{T} \sum_{k'=1}^{K} \sum_{g=1}^{G} x_{tk'g} + u_k \qquad k \in K \tag{18}$$

$$u_k \geq 0 \qquad k \in K \tag{19}$$

$$x_{tkg}, y_{tkg} \in \mathbb{Z}^+ \qquad t \in T;\ k \in K;\ g \in G$$

For each patient category k, a new decision variable u_k is defined. It measures the deviation from target level d_k for each $k \in K$ in terms of patient. While the treatment continuity (1) and capacity constraints (2) are preserved in (M), the patient mix requirements are enforced by new constraint sets (17) and (18). Although these two constraints allow model (M) to treat below and above the target levels for each category k, deviation from desired mixes is penalized in the objective function. Note that the model (M) aims to maximize the number of total fractions delivered and minimize the total deviations from patient mix ratios at the same time. In Section 3, a solution method for model (M) is provided to demonstrate the quantified tradeoffs between two objectives.

3 NISE Method

As with most integer programs, the exact construction of efficient frontiers is quite challenging. Therefore, we wish to study the structure of the efficient frontiers for a relaxed version of (M) in which the integrality restrictions are omitted. The generation of these frontiers can be accomplished through use of the so-called *Noninferior Set Estimation* (NISE) method. The ϵ-constraint and weighted sum methods are the two alternative methods that can be utilized to produce the noninferior set for problem (M). However, these methods need strong analyst intuition about the shape of the noninferior set. Hence, the NISE method has been shown to be more efficient in producing noninferior sets than its competitors [17]. The NISE method was first proposed by Cohon et al. [17, 18] and that generates the exact shape of the noninferior set that will allow us to examine the tradeoffs between the total patient mix deviations and the total number of fractions for the relaxation of our problem.

Before proceeding, we introduce the following notation notation used in presenting the NISE method. Let P_1 and P_2 be the optimal solutions that correspond to the maximum total patient deviation that can be observed and maximum total fractions, respectively. Furthermore, P_t is denoted as the t^{th} noninferior extreme point generated. Note that P_t and P_{t+1} are not necessarily adjacent in general. Therefore, ordering noninferior points is handled by defining the set S as the adjacent noninferior set of points and S_i as the i^{th} highest value of Z_2. Accordingly, the initial two points are sorted as $P_2 = S_1$ and $P_1 = S_2$. In the algorithm, Z_1 and Z_2 are defined as the objective function equations corresponding to the total patient mix deviation and total fractions. Subsequently, if $\bar{x}$ is given as a vector of decision variables then $Z_1(\bar{x})$ and $Z_1(\bar{x})$ generate the values of associated objective functions. The calculation of the weights assigned to these two objectives is based on the slope (α) of the line segment connecting S_i and S_{i+1}, where α is given by

$$\alpha = \frac{Z_2(S_i) - Z_2(S_{i+1})}{Z_1(S_i) - Z_1(S_{i+1})}. \tag{20}$$

By the definition of S and the nature of the noninferior set, Z_2 always decreases and Z_1 always increases as we move from S_i to S_{i+1}. Therefore, the slope α is always negative. Then, corresponding weights of two objectives should be chosen so that

$$\frac{w_1}{w_2} = -\alpha. \tag{21}$$

By letting $w_2 = 1$ and plugging (20) into (21), w_1 can be computed as follows;

$$w_1 = \frac{Z_2(S_i) - Z_2(S_{i+1})}{Z_1(S_{i+1}) - Z_1(S_i)} \tag{22}$$

Note that (22) is always positive. Then the weighted objective function of interest is

$$\max Z(\bar{x}; w_1, w_2) = \max w_1 Z_1(\bar{x}) + w_2 Z_2(\bar{x}) \tag{23}$$

which becomes (24) by substituting (22) and $w_2 = 1$

$$\max B_{i,i+1} = [Z_2(S_i) - Z_2(S_{i+1})](Z_1(\bar{x})) + [Z_1(S_{i+1}) - Z_1(S_i)](Z_2(\bar{x})). \tag{24}$$

Note that $B_{i,i+1}$ is the weighted objective function for the line segment between points S_i and S_{i+1}.

The maximum possible error, $\psi_{i,i+1}$, is defined with respect to the line segment connecting S_i and S_{i+1}. It can be calculated by measuring the maximum distance between the lower bound and upper bound over the segment. In other words, it is a perpendicular line to the lower bound and passing through the intersection of the two weighted objective function contours. In our implementation of the NISE method, we consider an error value less that 0.001 to be zero to address to address computational precision concerns. That is, initially, we begin with all $\psi_{i,i+1} = 1$ and the algorithm terminates if $\psi_{i,i+1} < 0.001$ for all adjacent noninferior points.

Finally, let $V_{i,i+1}$ be the value of $B_{i,i+1}$ evaluated at S_i and $S_{i,i+1}$, and $\bar{B}_{i,i+1}$ be the optimal value of $B_{i,i+1}$ when (24) is solved. If the solution of weighted problem leads to $\bar{B}_{i,i+1} = V_{i,i+1}$, then it means that S_i, S_{i+1} and line segments connecting them are in the noninferior set (e.g. $\psi_{i,i+1} = 0$). On the other hand, if $\bar{B}_{i,i+1} > V_{i,i+1}$, then a new feasible noninferior point has been found that lies above the current line segment.

Using the notation and definitions described above, we summarize the NISE algorithm in the following four main steps:

1. Initialize the algorithm by obtaining P_1 and P_2. Note that there might be inferior alternative optimal solutions to either of these problems. Make sure that P_1 and P_2 are noninferior solutions to Z_1 and Z_2, respectively. After computing the error ($\psi_{1,2}$), let $n = 2$ (n: number of distinct points currently in S).

2. If $\psi_{1,2} = 0$ for $i = 1, 2, ..., n-1$, then stop. Exact representation of the noninferior set is obtained for points S_i for $i = 1, 2, ..., n$ and the line segments connecting them. Otherwise go to step 3.

3. Pick a $\psi_{1,2} = 1$ corresponding the highest noninferior point in Z_2. Solve the weighted problem using the objective function in (24). If $\bar{B}_{i,i+1} = V_{i,i+1}$, then set $\psi_{1,2} = 0$ and return to step 2. If $\bar{B}_{i,i+1} > V_{i,i+1}$, label the new noninferior solution as P_{n+1} and go to step 4.

4. Reorder the points P_t, $t = 1, 2, ..., n+1$. Note that P_{n+1} has a value of Z_2 next highest after $Z_2(S_i)$. Therefore, relabel the points in set S as follows:

$$S'_t = S_t \qquad\qquad t = 1, \ldots, i$$

$$S'_{i+1} = P_{n+1}$$

$$S'_{t+1} = S_t \qquad t = i+1, \ldots, n.$$

Update error terms as follows:

$$\psi'_{t,t+1} = \psi_{t,t+1} \qquad t = 1, \ldots, i-1 \quad (\text{ if } i \geq 1)$$

$$\psi'_{t+1,t+2} = \psi_{t,t+1} \qquad t = i+1, \ldots, n-1 \quad (\text{ if i} \leq n-2).$$

Finally, compute $\psi'_{t,t+1}$ and $\psi'_{t+1,t+2}$. Increment n by 1 and return to step 2.

The NISE method is applied to obtain the efficient frontiers for each formulation described in Section 2. The frontiers reflect the impacts of side constraints on the capacity usage of the proton therapy facility in the case of varying patient mix deviation levels. The obtained results are discussed in Section 4 in detail.

4 Computational Study

In this section we present a computational study for the bicriteria model defined in Section 2.3. Our study focuses on the generation of efficient frontiers for the LP-relaxation of model (M). The results of this section clarify the tradeoffs between total number of fractions treated and total patient mix deviations in a proton therapy facility for a finite planning horizon. Section 4.1 discusses the instance generation scheme for this study. In the remaining sections, we discuss the relationships between the capacity usage and corresponding deviation of the patient mix constrains from the target levels in the presence of different operational constraints mentioned in Section 2.

4.1 Experimental Design

Table 1 provides the parameters used in the set of instances in considered in our computational tests. Our investigation includes instances with 3 different patient mix ratios (PMRs), 2 different capacity levels of gantries ($C_{tg} = C = 12$ and 15 hours) and 7 planning period lengths ($T = 75$, 100, 150, 200, 300, 400, and 500 days). For each PMR, common patient category parameters $(c_k, \bar{c}_k, f_k, n_k)$, shown in Table 1, are used. In Section 4.2, we discuss the effects of adding each operational side constraint presented in Section 2.2 to the base model individually. Consequently, the figures provided refer to the frontiers drawn according to the corresponding constraint or model name (e.g. "Base model frontier", "Anesthesia frontier").

Table 1: Parameters of Patient Categories

	Patient Categories									
	1	2	3	4	5	6	7	8	9	10
PMR1	0.10	0.10	0.10	0.10	0.10	0.10	0.10	0.10	0.10	0.10
PMR2	0.20	0.10	0.20	0.10	0.05	0.10	0.05	0.10	0.05	0.05
PMR3	0.65	0.15	0.07	0.03	0.03	0.02	0.01	0.01	0.02	0.01
f_k (# of fractions per day)	1	1	2	2	1	1	1	1	1	1
n_k (min)	40	40	31	31	30	30	30	30	42	12
c_k (min)	18	30	35	45	35	55	60	90	50	35
$\bar{c}_k$ (min)	15	15	20	25	20	20	45	45	30	20
BID Patients	-	-	✓	✓	-	-	-	-	-	-
Anesthesia Patients	-	-	-	-	-	✓	-	✓	-	-
Specialize Gantry 3 for	✓	-	-	-	-	-	-	-	-	-

The restrictions imposed by operational constraints are also summarized in Table 1. Patients from categories 3 and 4 need to be treated twice in a day (BID). Therefore, the corresponding f_k values are 2 for these patient categories. Even though the time requirement between 2 treatment sessions (τ) is assumed to be 6 hours, we discuss the impacts of this time interval in detail in Section 4.4. Separately, the anesthesia team is required while treating patients from 6^{th} and 8^{th} categories. The default value of the anesthesia team availability (A_g) in the facility is 4 hours in a single gantry (1×4). In addition, we study the impacts of this availability for different levels in Section 4.3. In Section 4.5, we discuss the effects of specializing gantry 3 such that it may only treat patients from category 1, as well as the interactions between the gantry switching flexibility and gantry specialization constraints. Section 4.6 includes discussion about prime hours restrictions. Accordingly, new patients are allowed to receive their treatment on Monday, Tuesday and Wednesday during prime hours from 9:00 am to 4:00 pm ($\eta_g = 420$ min).

The above instances were solved by using CPLEX 12.1 on a Microsoft Windows Server 2003 R2 with 2.93 GHz.

Frontiers presented in Section 4.2–Section 4.6 are plotted with default parameters ($C = 12$ hrs and $T = 75$ days) unless otherwise stated. For some figures, a second plot is drawn directly below the original one (e.g. see Figure 1) in order to identify the differences among frontiers by zooming in the parts that are hard to differentiate. Finally, the effects of gantry capacity and length of the planning period in case of different operational restrictions are discussed in Sections 4.7 and 4.8, respectively.

4.2 General Comparison of Frontiers

Figure 1 shows the behaviors of three operational restrictions; anesthesia, BID and gantry specialization constraints together with the base model. It should be noted that all of the frontiers are obtained in the absence of gantry switching flexibility unless stated otherwise. Again, this means that if the initial treatment of a patient is delivered in gantry g, subsequent fractions must also be delivered in same gantry g where the treatment is started. Plots in the first row of Figure 1 demonstrate the noninferior breakpoints and line segments for base model and operational restrictions in the case of three different patient mix ratios. The second row of Figure 1 captures the relationships of noninferior points and line segments for different operational constraints when the total deviation is smaller than 140. Note that the total number of patients and total number of fractions are not the same in a planning period. All n_k, and some f_k, values are strictly greater than 1. This means that the number of fractions is greater than the total number of patients for a given planning period. Moreover, the capacity, BID and anesthesia constraints are all quantified according to number of fractions. Therefore, total fractions is used on y-axis, rather than total patients. This value is plotted against total deviation on the x-axis. It should also be noted that total deviation is in terms of total number of patients not fractions.

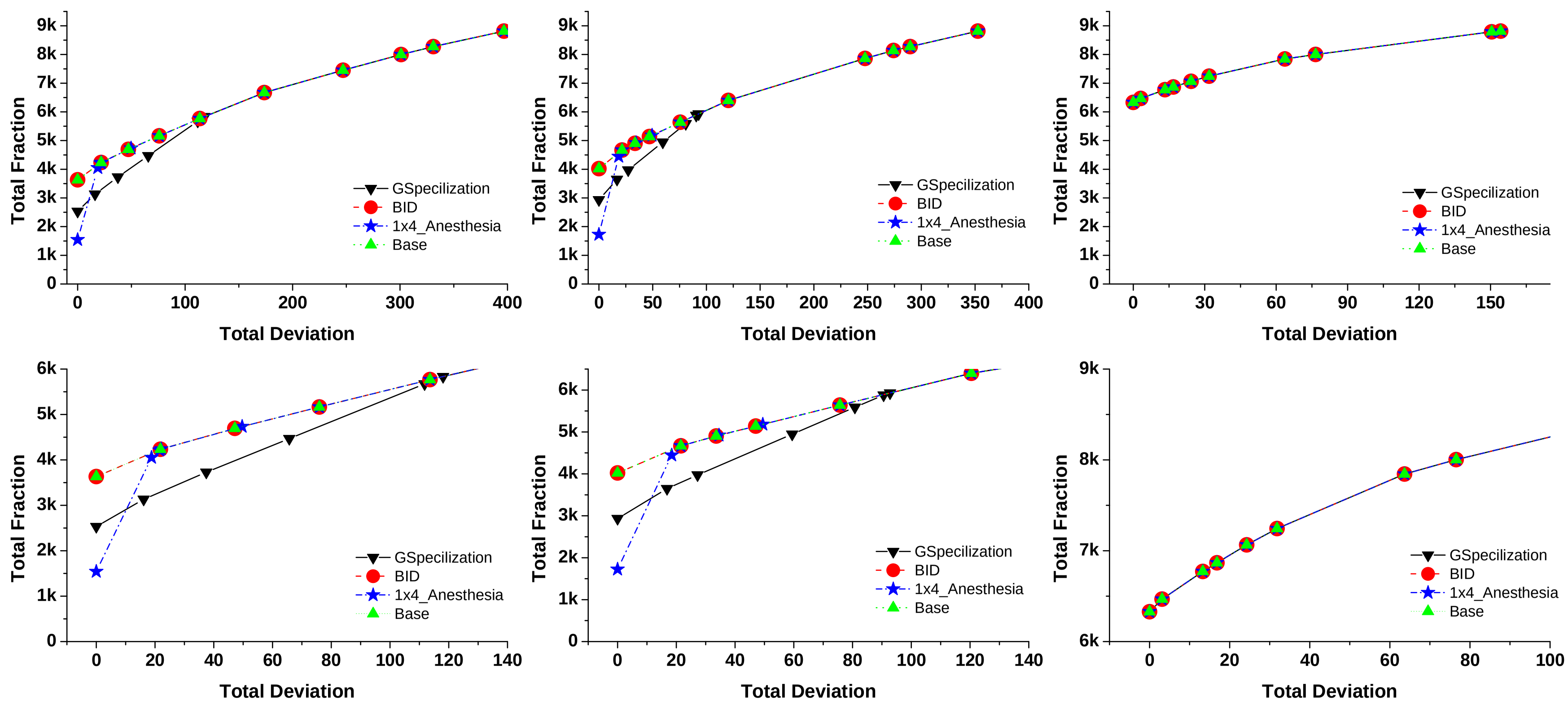

(a) PMR1 (b) PMR2 (c) PMR3

Figure 1: Impacts of operational restrictions

As shown in Figures (1a), (1b) and (1c), base model frontiers have the highest total number of fractions for a given amount of total deviation compared to other operational constraints, regardless of the patient mix ratios in use. This is because, it is the simplest (relaxed) version among all formulations. However, after a certain amount of total deviation, all operational constraint frontiers tend to merge with the base model frontiers. The reason behind this inference is that as the total deviation increases, the impacts of operational restrictions disappear. If the actual patient mix ratio of category k is greater than the target level (d_k), it means that the resources reserved for other categories are used to treat patients from category k. In other words, treating fewer patients than the target levels from categories which are exposed to additional restrictions (BID, anesthesia availability, gantry specialization) leads to higher totals of fractions treated when compared to cases where the target levels are satisfied (total patient mix deviation is 0). This is interpreted as the higher the total deviation, the smaller the impact of operational restriction. However, more complicated relationships behind the scene are revealed by further investigations in the following sections.

4.3 Anesthesia Frontiers

In Figures (1a) and (1b), it can be seen that after a small deviation of 21.56, anesthesia break points are aligned with the base model frontiers since the deviations are used to treat more patients from categories other than 6 and 8 (anesthesia patients). Note that number of patients treated in these categories become 0 after total deviation reaches 113.63. This fact can be seen in Figure 2, which demonstrates the change in actual mix ratios of each patient category with corresponding total deviation in the case of PMR1 and PMR2. As expected, actual mix ratios are exactly equal to the target mix ratios for each category, regardless of the patient mix ratio, when the total deviation is zero. However, the number of treated patients from patient category 8 is 0 when the total deviation is 21.56 for the two frontiers associated with PMR1 and 2, whereas patients from category 6 are treated until the total deviation amount of 75.94 and 75.70 in case of PMR1 and PMR2, respectively. Note that the resources gained from the 6^{th}, 7^{th} and 8^{th} categories are used to treat patients from the 1^{st} and 3^{rd} categories which are more attractive in terms of treatment duration (c_k) and patient setup time ($\bar{c}_k$). Also, our results suggest that a higher treatment and patient setup time, together with the patient mix constraints, make anesthesia constraints highly restrictive. In Figures 1a and 1a, it is seen that the anesthesia availability restriction remains active until a total deviation amount of 25. Note that anesthesia availability in gantries does not only impact the number of fractions delivered to these categories. It also limits the number of non-anesthesia patients due to patient mix requirements enforcing that the number of patients treated from any category must be proportional to others according to PMR in use. As a consequence, the availability of the anesthesia team has significant impacts on the number of fractions delivered to non-anesthesia categories as well since patient mix constraints indirectly keep the total patients from all categories proportional to each other. However, as the total deviation increases, this indirect restriction is removed and anesthesia frontiers are aligned with the base model frontiers.

Figure (1c) reveals that 4 hours of anesthesia availability in a single gantry (1×4)

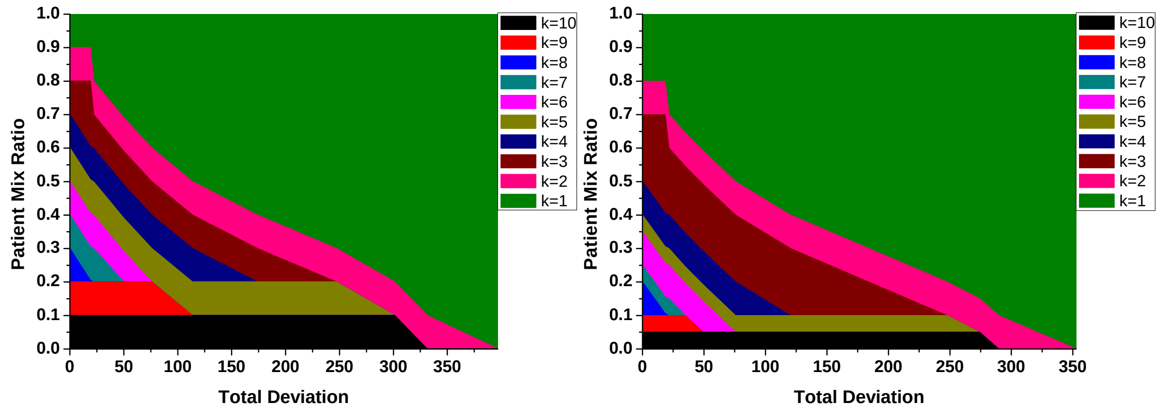

(a) PMR1

(b) PMR2

Figure 2: Stacked area representation of Table 1

has no impact on other patient categories due to small patient mix ratios of anesthesia patient categories (see Table 1). In other words, the percentage of anesthesia patient categories are so small that 4 hours of anesthesia team availability is enough to serve all anesthesia patients implied by any patient mix ratios. For PMR3, in order to have noninferior points and line segments for anesthesia frontiers different from the base model, either: (i) patient mix ratios of categories 6 and 8 should be increased or (ii) the duration of the anesthesia team availability should be decreased to make anesthesia constraints more restrictive. Further investigations are made to capture the relationship between the anesthesia and patient mix constraints in the following section.

4.3.1 Impacts of Anesthesia Availability Hours

Impacts of anesthesia availability can be clearly seen in Figure 3. Anesthesia availability in a single gantry is varied from 4 hours through 8 hours (1×4,1×6 and 1×8)

and impacts of capacity increase in relationship to base case are demonstrated on Figures (3a) and (3b) in case of PMR1 and PMR2, respectively. It is observed that

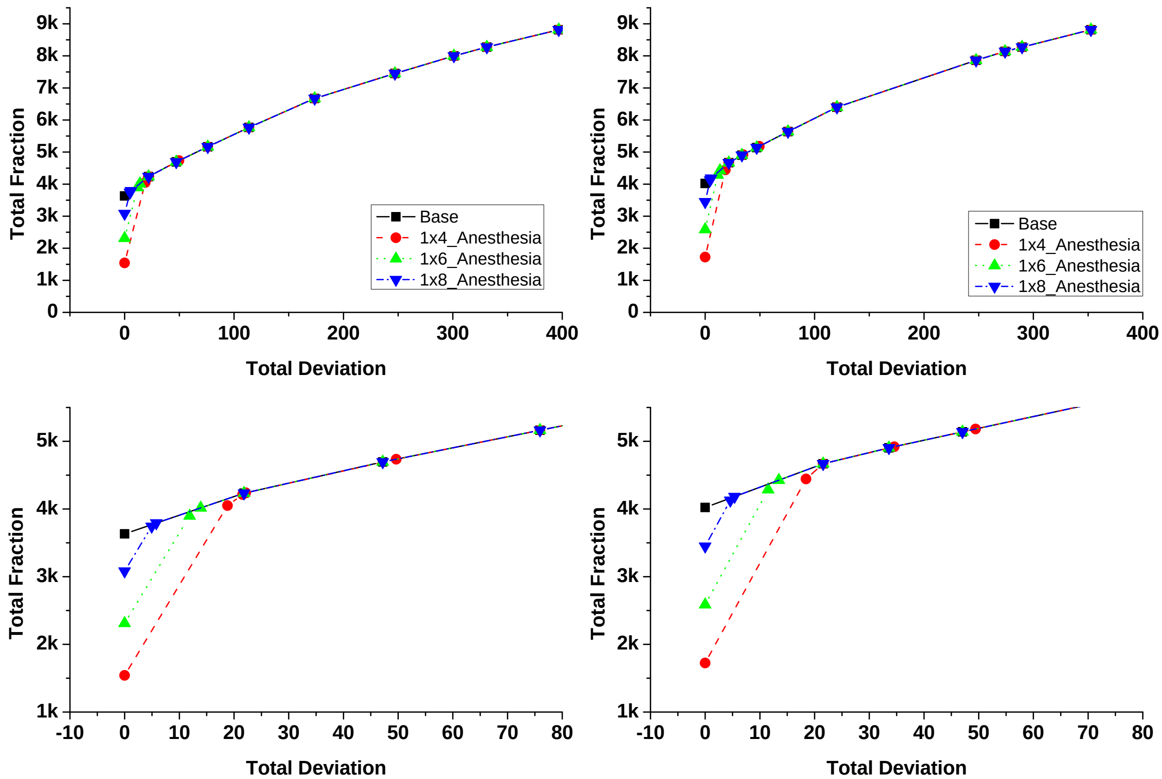

(a) PMR1 (b) PMR2

Figure 3: Impacts of anesthesia availability in gantries

additional anesthesia availability increases the total number of fractions delivered in a planning period dramatically. This is particularly true when the total deviation is small. For instance, increasing anesthesia availability 2 hrs (1×6) and 4 hrs (1×8) reduces the matching point of anesthesia and base model frontiers on the x-axis from 25 to 15 and 5, respectively (see Figure 3). Knowing that treatment and patient setup durations are kept constant, as shown in Table 1, the number of treated anesthesia patients is increased for a given level of deviation. This allows the gap between base model and anesthesia frontiers to close as the total deviation allowed increases as seen in both Figures (3a) and (3b).

4.4 BID Frontiers

Figure 1 points out that the time difference between two sessions of BID patients (τ= 6 hrs) is adequate to treat as many fractions as in the base case, regardless of patient mix ratio. For this case, noninferior points and line segments obtained by NISE method for both BID and base formulations are identical. Although 6 or 8 hour rest periods between twice-daily treatment sessions is adequate to allow complete repair on healthy tissues, there might be some cases where interfraction interval time is required more than 8-hours [19]. Hence, from a management perspective, it is vital to see the impacts of different interfraction intervals (τ=6, 9, 10 hrs) on the number of total fractions from all categories within allowed deviations from patient mix constraints.

Noninferior set approximations by NISE method for different PMRs and interfraction intervals can be seen in Figure 4. From Table 1, the total mix ratio for BID patient categories (3 and 4) is 20%, 30% and 10% in case of PMR1, 2 and 3, respectively. Since PMR2 has the highest mix ratio of BID patients, frontiers in Figure 4b are more sensitive to a change in interfraction interval. However, for each PMR (see Figures (4a), (4b) and (4c)), it is indicated that for a 10-hour rest period obligation, the total fractions delivered in a planning period is dramatically decreased due to BID constraints. This is illustrated clearly when the total deviation is around 50 for PMR1 & 2 and 5 for PMR3. On the other hand, even though a 9-hour rest period has less impact on total fractions, compared to 10-hour interval, BID constraints become

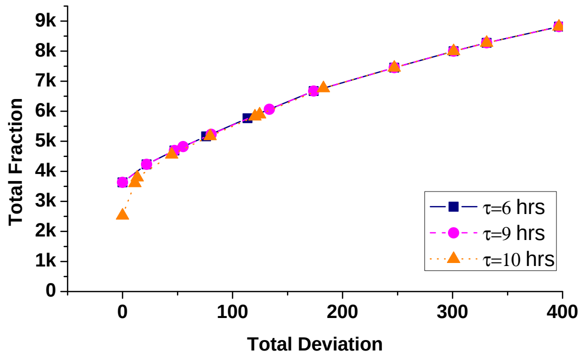

(a) PMR1

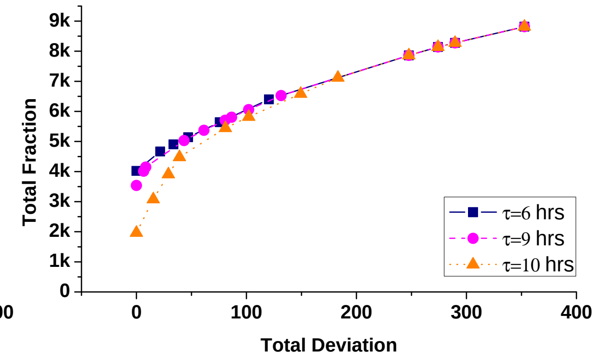

(b) PMR2

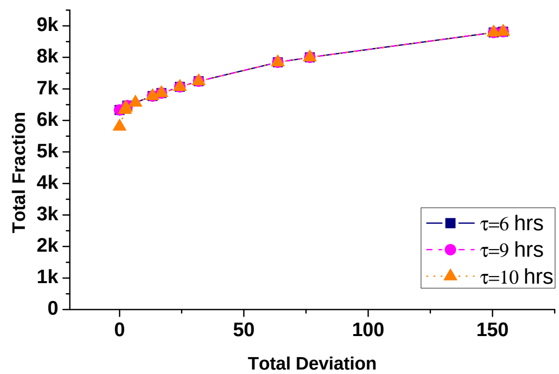

(c) PMR3

Figure 4: Impacts of τ on total fractions

tight for PMR2 where total mix ratio of BID patients is 30%. 9-hour rest period has slightly changed the coordinates of noninferior points in case of PMR1. However, this is not significant due to the fact that noninferior line segments on both base and BID formulation frontiers are nearly identical. Even though the coordinates of breakpoints are different, boundaries of noninferior sets are approximately same.

4.5 Gantry Specialization Frontiers

Gantry specialization requires restricting the use of the 3^{rd} gantry for only patients from 1^{st} category. Figures (1a) and (1b) point out that this is a restrictive constraint since patient mix percentages for the 1^{st} category are only 10% and 20 % in PMR1 and 2, respectively. However, it does not alter total fractions when compared to the base model in use of PMR3. This follows due to the fact that the 1^{st} patient category has a mix of 65% and it is worthwhile to reserve a gantry for this amount of fractions from 1^{st} category. On the other hand, specializing gantry 3 for only patients from 1^{st} category in case of PMR1 and 2 is not only wasting the reserved capacity for gantry 3, it also significantly limits the available capacity for other patient categories as well. As a consequence, less amount of fractions are treated than the base case model when the total deviation is smaller than 118.06 (PMR1) and 90.57 (PMR2).

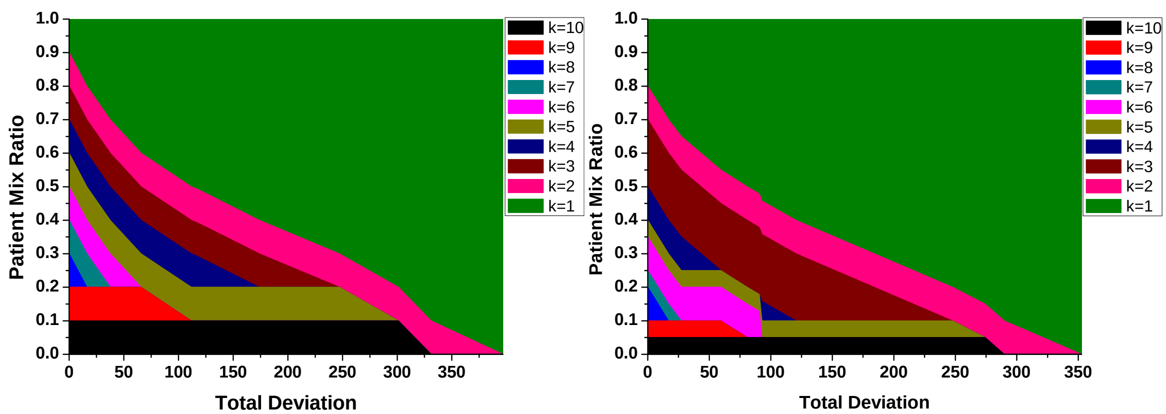

(a) PMR1 (b) PMR2

Figure 5: Actual patient mix percentages for gantry specialization frontiers

Figure 5 demonstrates actual patient mix percentages for PMR1 and PMR2. At this point, a majority of the deviation is consumed by the 1^{st} patient category to treat more 1^{st} category patients in order to fully use the allocated capacity to this category in gantry 3.

It should be highlighted that specializing gantry 3 for only patient category 1 does not force patients from 1st category not to be treated in other gantries. It only prevents treatment of patients from different categories other than 1^{st} one in gantry 3. Hence, investing total deviation on the 1^{st} patient category from the 6^{th} breakpoint forward does not necessarily mean that these patients need to be treated in the specialized gantry. Other two gantries are still open to patients from 1^{st} category as well.

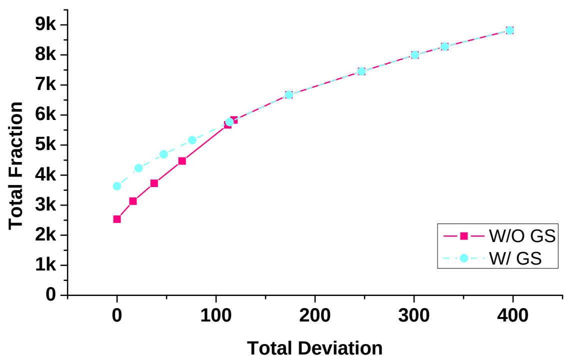

(a) PMR1

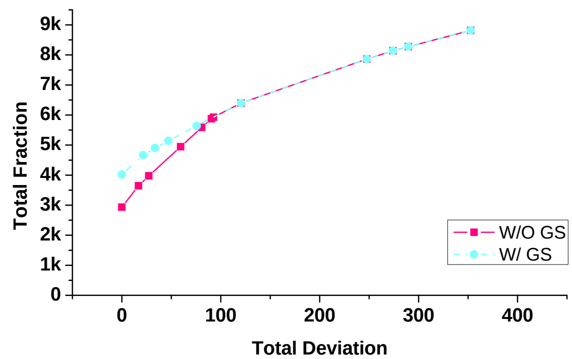

(b) PMR2

Figure 6: Impacts of gantry switching flexibility

It is also important to see the reactions of gantry specialization constraints to gantry switching flexibility. This is because prohibiting gantry switching only impacts gantry specialization frontiers. Other formulation frontiers (BID,Anesthesia, etc.) are not affected by gantry switching flexibility. Therefore, the NISE method is used to draw the gantry specialization frontiers in the presence of gantry switching flexibility and the results are shown in Figure 6. Regardless of patient mix ratio, gantry switching flexibility makes gantry specialization and base model frontiers identical since it removes the obstacle preventing treatment of patient gantries in gantry 1 other than the 1^{st} category patients.

4.6 Prime Hours Frontiers

Figure 7 provides insights into the impacts of prime hours constraints in the case of 3 different PMRs considered. Even though new patients can only be accepted in the first three weekdays, a small gap is observed between prime hours and base model frontiers in use of each PMR. Interestingly, prime hours and base model frontiers appear aligned for a small amount of allowed total deviation. However, as shown In Figures (7a) and (7b), the gaps between the frontiers become visible after a total deviation amount of 250. This threshold is approximately 60 in Figures (7c) for PRM3.

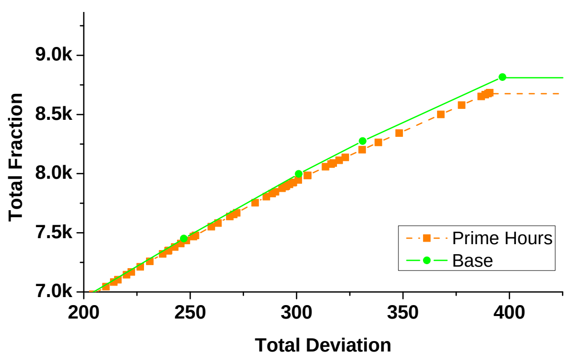

(a) PMR1

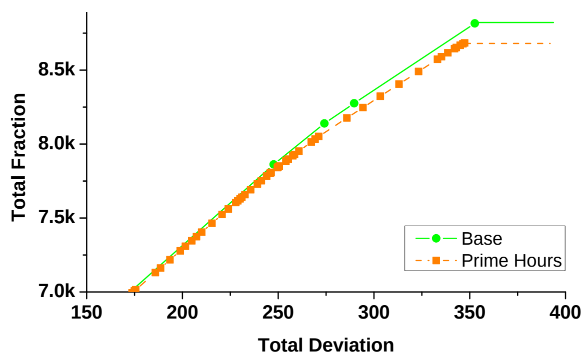

(b) PMR2

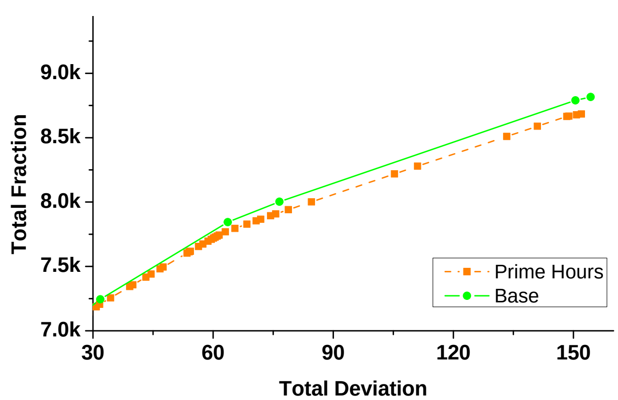

(c) PMR3

Figure 7: Impacts of Prime Hours Constraints

Note that previous operational restrictions (anesthesia availability, BID and gantry specialization) create additional capacity restrictions based on different patient categories. Anesthesia team availability, BID and gantry specialization constraints limit the capacity of treating patients from corresponding categories. In addition to the time limit (η_g) on treating new patients, prime hours constraints also restrict accepting new patients from all categories on specified days. It is observed in the previous results that the model overcomes extra capacity constraints by deviating more and more from the target levels. For the prime hours constraints, this strategy appears to be effective until a certain amount of total deviation is attained (see Figures (7a), (7b), (7c)). However, a fewer number of total fractions are delivered when compared to base model frontiers as the deviation increases.This is because of the fact that deviating from target levels becomes less beneficial compared to the base model since the overall number of patients is already limited by prime hours constraints.

Another important property of prime hours frontiers is the dramatically increased number of breakpoints compared to other frontiers. Prime hours constraints differentiate the days of the planning periods by introducing T_{NA} as the first 3 days of weeks. As a consequence, the NISE method produces frontiers with greater number of breakpoints for the altered set T that includes nonidentical days.

Finally, we introduced the constraints in Section 2.2.4 to the base model with prime hours constraints in order to gain more flexibility over constraints (9). However, no improvement is obtained in terms of total fractions even though capacity exchange is allowed among gantries on specified days. This is because of the fact that the maximum number of patients can be treated is strictly restricted by constraints (10) and (9) for a finite planning period. In addition, capacity exchange among gantries do not save more time for additional patients outside of bringing flexibility on treatment schedules.

4.7 Impacts of Gantry Capacities

In this section, we discuss the impacts of increasing daily gantry capacities from 12 hrs to 15 hrs. As expected, increasing C while keeping other patient category parameters ($\bar{c}_k$, c_k, etc.) constant results in delivering more fractions for a given total deviation (see Figures 8, 9, 13 and 14).

Figure 8 demonstrates the impacts of raising daily capacities 3 more hrs on anesthesia frontiers. Discussion in Section 4.3.1 highlights the relationships between anesthesia availability and patient mix constraints. Recall that patient mix constraints indirectly limits the number of non-anesthesia patients while PMR1 and PMR2 are in use. In case of PMR3, total mix of anesthesia patients is 3%. Therefore, 4 hrs of anesthesia team availability is enough to serve all anesthesia patients and other categories are not restricted by patient mix constraints. Analogously, as seen in Figures (8a) and (8b), raising daily capacities 3 hrs per day does not lead to any increase in number of total fractions until a total deviation of 25 in case of PMR1 and 2. As the total deviation increases (> 25), indirect impacts of patient mix ratios disappear. Immediately after that deviation threshold, frontiers begin to diverge from each other and the total number of fractions are improved by the 3 hour capacity increase on each gantry.

Figure 9 demonstrates the impacts of the increase in daily capacities of 3 gantries

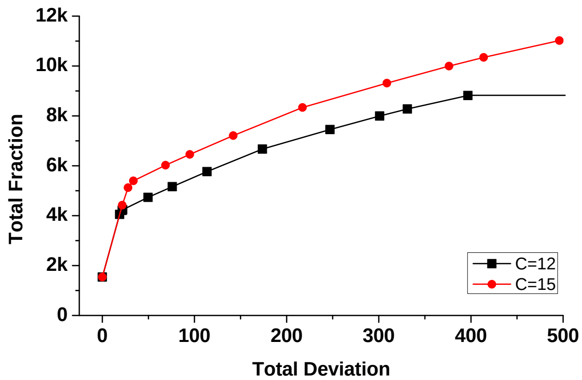

(a) PMR1

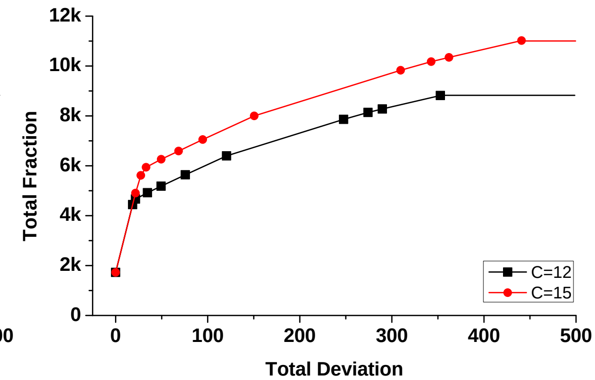

(b) PMR2

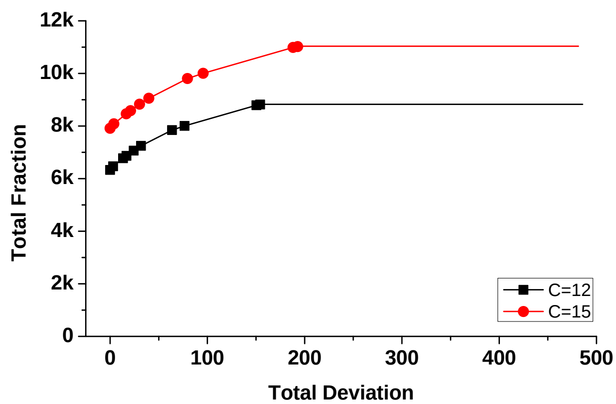

(c) PMR3

Figure 8: Impacts of C on anesthesia frontiers

from 12 hours to 15 hours on gantry specializing frontiers. In Section 4.5, for PMR1 and PMR2, it is shown that specializing gantry 3 for the 1^{st} patient category makes gantry 3 primarily idle. Recall that as the total deviation is used to treat more patients from this category, utilization of gantry 3 is increased and gantry specialization frontiers are aligned with those generated for the base model. Similarly, the gain in terms of total fractions is reflected on frontiers in Figures (9a) and (9b) after the 1^{st} gantry is fully utilized. Until these levels in both figures, capacity increase in gantry 2 and 3 explain the gap between frontiers corresponding to $C = 12$ hours and $C = 15$ hours. Note that for PMR3, since 65% mix ratio of 1^{st} patient category keeps the utilization of gantry 3 high, the increase in daily gantry capacity improves the total fractions regardless of the total deviation level (see Figure 9c).

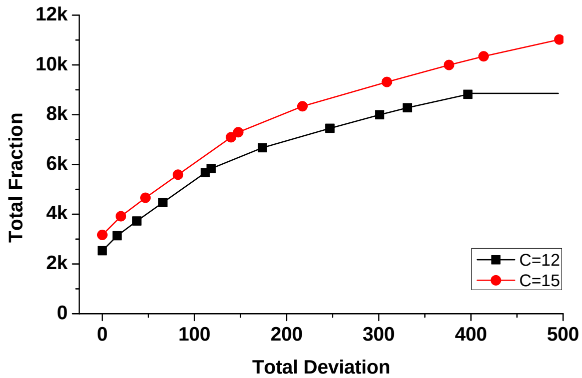

(a) PMR1

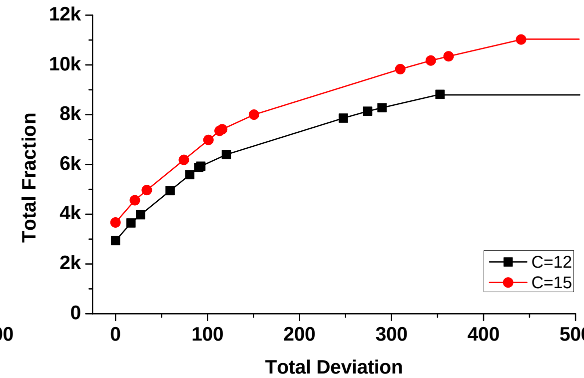

(b) PMR2

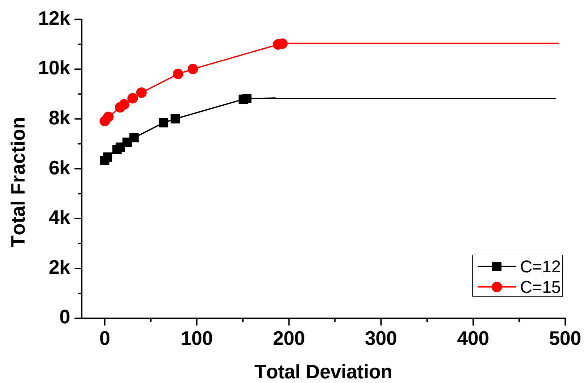

(c) PMR3

Figure 9: Impacts of C on gantry specializing frontiers

4.8 Normalized T Frontiers

In this section, we discuss the impacts of using different period planning length. We gradually increase T from 75 to 500 days and produce efficient frontiers for each stage of T. As expected, increasing T while keeping other patient category parameters (n_k, c_k, etc.) constant yields in delivering more fractions for a given total deviation (see Figures 15, 16, 17 and 18). In order to possess the impacts of planning period length, we scaled each of the curves by dividing both total deviation and fraction values by T and obtained normalized T plots as seen in Figures 19 and 20. It was observed that normalized T frontiers for each formulation overlap for the cases where planning period length is greater than or equal to 75 days. However, the exact value of T at where the convergence has essentially taken place still needs to be identified. Hence, other normalized plots with $T \leq 75$ are also drawn for each formulation as well.

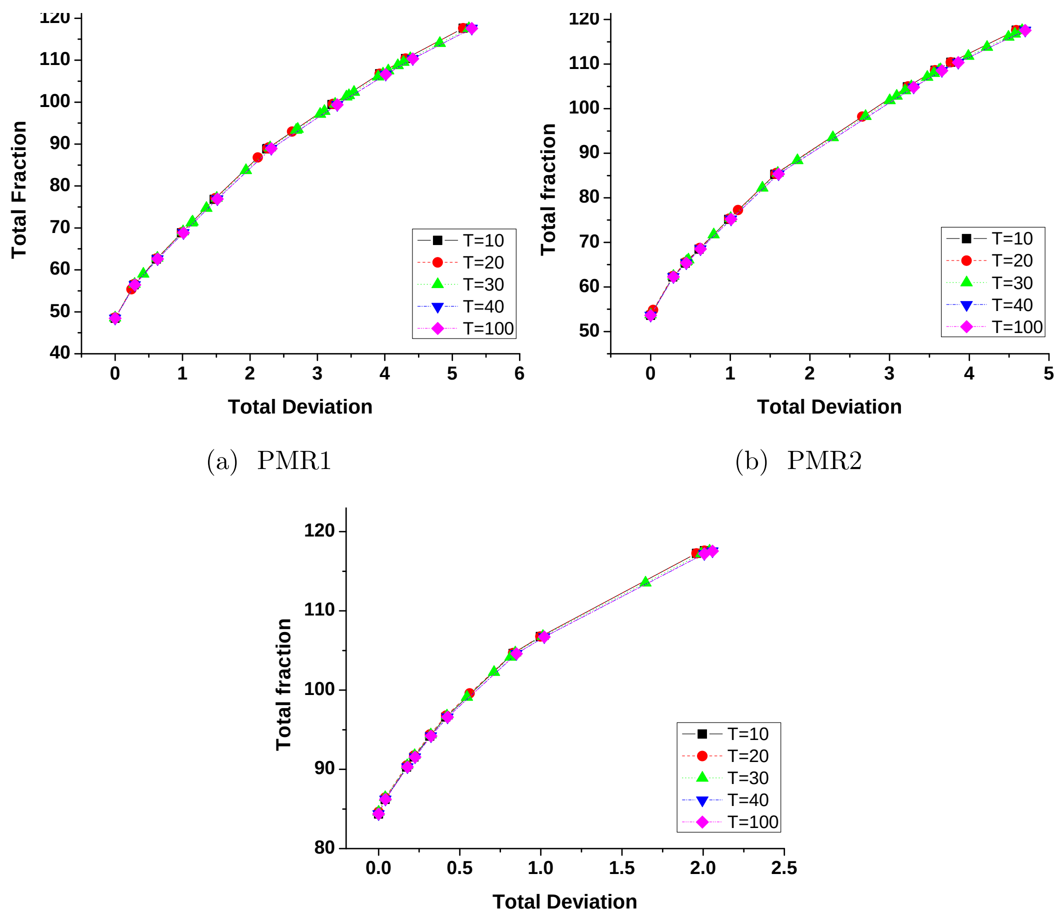

(a) PMR1 (b) PMR2

(c) PMR3

Figure 10: Normalized T base model frontiers

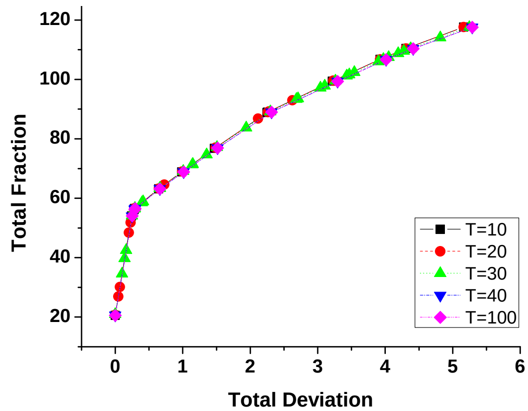

(a) PMR1

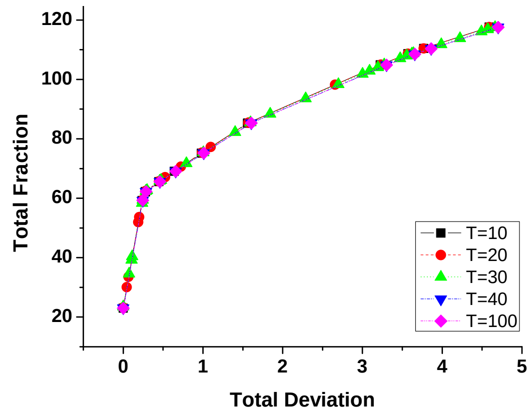

(b) PMR2

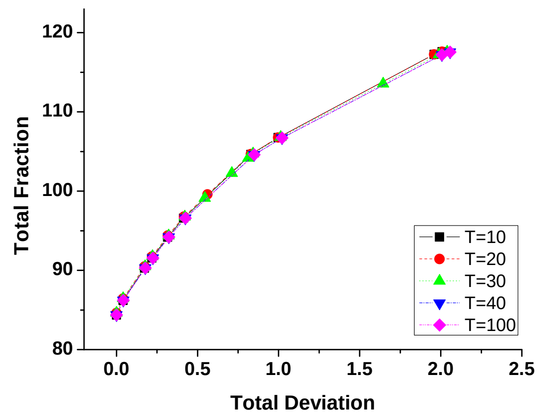

(c) PMR3

Figure 11: Normalized T anesthesia frontiers

Figures 10, 11 and 12 demonstrate normalized T frontiers for base model, anesthesia and gantry specialization operational constraints, respectively. Three dimensional representation of these plots can be seen in Figures 21, 22 and 23. Even though the frontiers coincide when the total deviation is small, they start to differ from each other when the total deviation gets larger. For instance, number of breakpoints increases dramatically when $T = 20$ and $T = 30$ as the deviation gets larger. However, both the noninferior points and line segments connecting them become identical for $T = 40$ and $T = 100$. Since, the frontiers are aligned with each other for $T \geq 75$ (see Figures

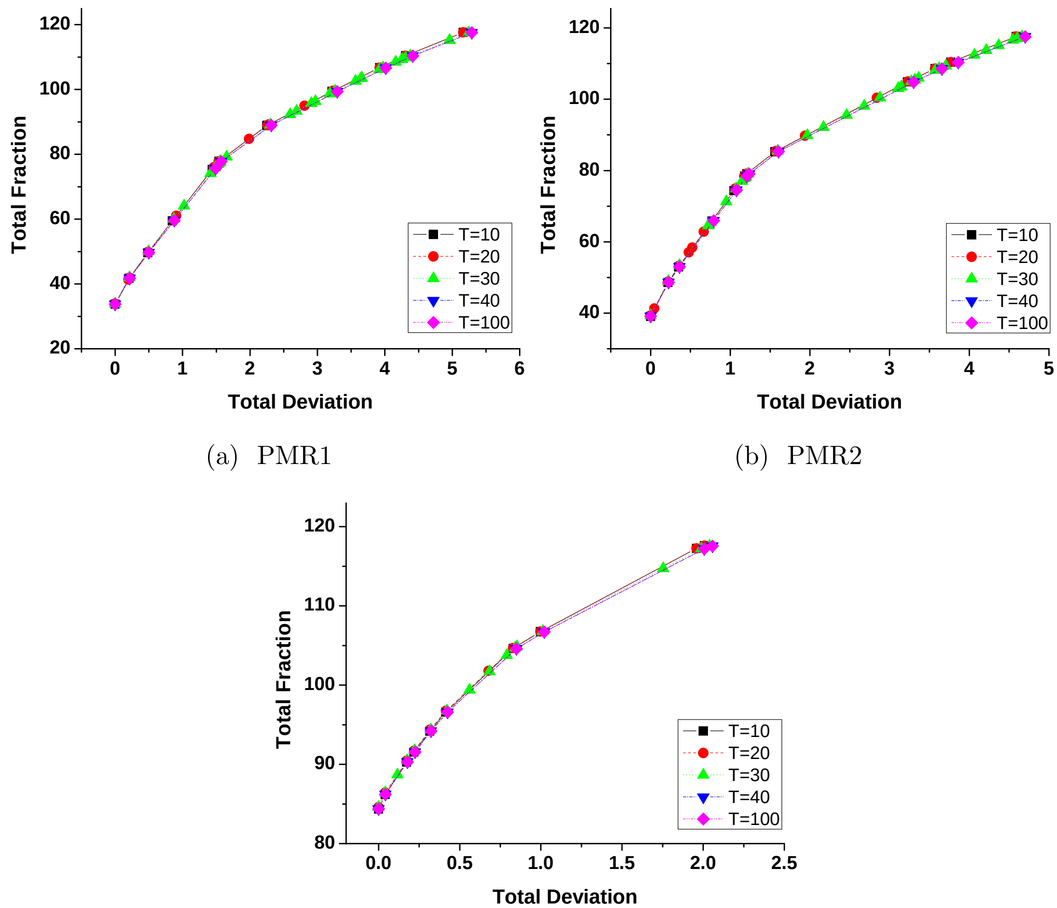

(a) PMR1

(b) PMR2

(c) PMR3

Figure 12: Normalized T gantry specialization frontiers

19 and 20) and the curves for $T = 40$ and $T = 100$ are indistinguishable, we can conclude that $T = 40$ is a sufficient planning period to capture all effects consistently among the model variants.

5 Conclusion & Future Work

In this thesis we explored the impacts of operational limitations on the proton therapy facility in light of strategic patient mix constraints. We began by describing commonly encountered problems and general solution methodologies in the healthcare scheduling environment in Section 1. After defining our problem with its unique elements in Section 2, we proposed a general IP model (M) with three vital constraints in Section 2.1. It was observed that the combination of integrality restrictions and patient mix constraints, the problem was quite difficult to solve in order to make strategic decisions. Subsequently, our research focused on the relaxed version of a bicriteria representation of the problem, (M), which considers tradeoffs between deviations from patient mix preferences and their impacts on the capacity.

Our study provides insights for MDMs via projected limitations on the proton therapy treatment capacity from common operational requirements coupled with strategic patient mix requirements. In Section 4, the frontiers obtained by NISE method for each formulation are piecewise-linear concave increasing functions. As expected, an increased allowable deviation from patient mix constraints can be used to treat additional patients from categories with smaller setup and treatment durations. Therefore, managers can utilize the results of our research to quantify the marginal cost of a fraction in terms of deviation from strategic target levels. In case of various deterministic demand patterns, the methodology is easily implemented so that forecasting scenarios for different PMRs can be portrayed accordingly. Therefore, healthcare planners can see the impacts of staff/patient scheduling and resource planning decisions and make necessary changes beforehand.

As observed from frontiers generated in Section 4, total fractions treated is highest in base model frontiers (without additional operational constraints) for a given level of total deviation. However, as the allowable patient deviation increases, patient mix requirements become less restrictive. After a certain amount of total deviation, all frontiers begin converging and the cost of increasing total fraction by one unit becomes more and more expensive. Some patient categories (i.e. BID, anesthesia, gantry specialization) are susceptible to specialized operational constraints. For categories limited by these additional restrictions, the percentage of patients treated decrease below target levels. When the total deviation amount is not able to compensate the additional operational limitation (< 30 for anesthesia frontiers, < 100 for gantry specialization frontiers, etc.), the impacts of patient mix constraints become significant. This is because the impacted patient categories also lead to a decrease in number of patients treated from other categories due to proportional target levels. Hence, once the operational restriction influences patient categories, managers must account for the impacts of patient mix constraints as well. For a majority of the time, a small increase in the available resources results in decreased total deviation together with a substantial increase in total fractions (e.g. see Figures 3, 4).

References

[1] U. of Texas M. D. Anderson Cancer Center, "Proton therapy center opens to patients." http://www.medicalnewstoday.com/articles/46788.php, July 2006.

[2] M. Goitein and M. Jermann, "The relative costs of proton and x-ray radiation therapy," *Clinical Oncology*, vol. 15, pp. S37–S50, 2003.

[3] Y. Yamada, I. Ackerman, E. Franssen, R. G. Mackenzie, and G. Thomas, "Does the dose fractionation schedule influence local control of adjuvant radiotherapy for early stage breast cancer," *International Journal of Radiation Oncology, Biology, Physics*, vol. 44, pp. 99–104, 1999.

[4] W. Shelley, M. Brundage, C. Hayter, L. Paszat, S. Zhou, and W. Mackillop, "A shorter fractionation schedule for postlumpectomy breast cancer patients," *International Journal of Radiation Oncology, Biology, Physics*, vol. 47, pp. 1219–1228, 2000.

[5] B. Cardoen, E. Demeulemeester, and J. Bëlin, "Operating room planning and scheduling: A literature review," *European Journal of Operation Research*, vol. 201, pp. 921–932, 2010.

[6] J. Bowers and G. Mould, "Ambulatory care and orthopaedic capacity planning," *Health Care Management Science*, vol. 8, pp. 41–47, 2005.

[7] T. Cayirli, E. Veral, and H. Rosen, "Designing appointment scheduling systems for ambulatory care services," *Health Care Management Science*, vol. 9, pp. 47–58, 2006.

[8] D. N. Pham and A. Klinkert, "Surgical case scheduling as a generalized job shop scheduling problem," *European Journal of Operation Research*, vol. 185, pp. 1011–1025, 2008.

[9] D. Conforti, F. Guerriero, and R. Guido, "Optimization models for radiotherapy patient scheduling," *4OR*, vol. 6, pp. 263–278, 2008.

[10] D. Conforti, F. Guerriero, and R. Guido, "Non-block scheduling with priority for radiotherapy treatments," *European Journal of Operation Research*, vol. 201, pp. 289–296, 2010.

[11] S. M. Ballard and M. E. Kuhl, "The use of simulation to determine maximum capacity in the surgical suite operating room," *Proceedings of the 2006 Winter Simulation Conference*, pp. 433–438, 2006.

[12] B. Cardoen and E. Demeulemeester, "Capacity of clinical pathways a strategic multi-level evaluation tool," *Journal of Medical Systems*, vol. 32, pp. 443–452, 2008.

[13] S. Chaabane, N. Meskens, A. Guinet, and M. Laurent, "Comparison of two methods of operating theatre planning: Application in belgian hospitals," *Journal of Systems Science and Systems Engineering*, vol. 17(2), pp. 171–186, 2008.

[14] G. C. Kaandorp and G. Koole, "Optimal outpatient appointment scheduling," *Health Care Management Science*, vol. 10, pp. 217–229, 2007.

[15] P. M. V. Bosch and D. C. Dietz, "Minimizing expected waiting in a medical appointment system," *IIE Transactions*, vol. 32, pp. 841–848, 2000.

[16] M. Mulholland, P. Abrahamse, and V. Bahl, "Linear programming to optimize performance in a department of surgery," *J Am Coll Surg*, vol. 200, pp. 861–868, 2005.

[17] J. L. Cohon, R. L. Church, and D. N. Sheer, "Generating multiobjective tradeoffs: An algorithm for bicriterion problems," *Water Resources Research*, vol. 19, pp. 1001–1010, 1979.

[18] J. L. Cohon, *Multiobjective Programming and Planning*. Dover, 2003.

[19] I. F. Tannock, R. P. Hill, R. G. Bristow, and L. Harrington, *The Basic Science of Oncology*. McGraw-Hill, 2005.

6 APPENDIX

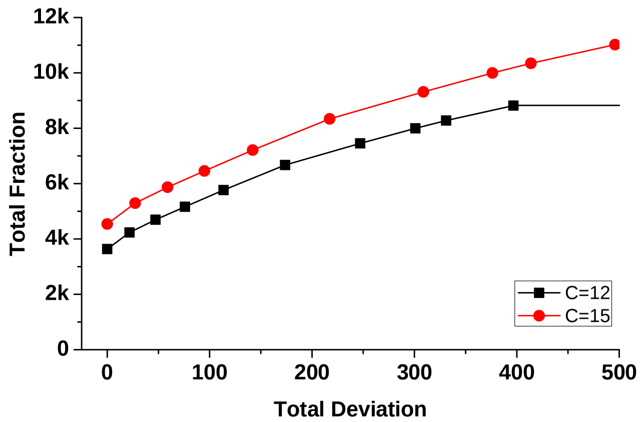

(a) PMR1

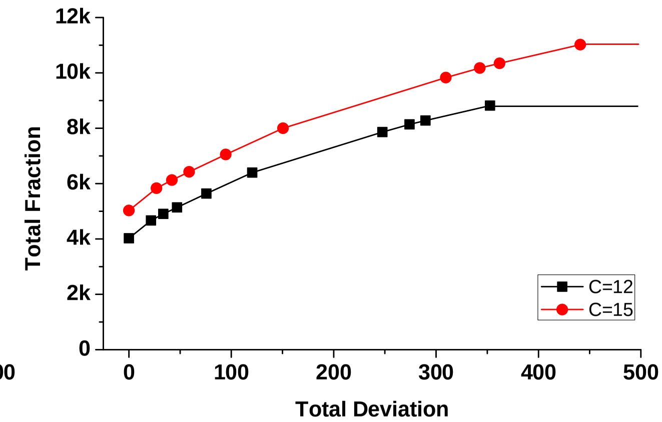

(b) PMR2

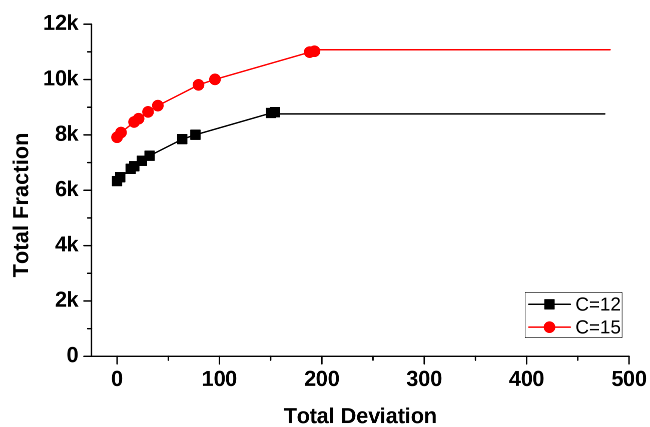

(c) PMR3

Figure 13: Impacts of C on base model frontiers

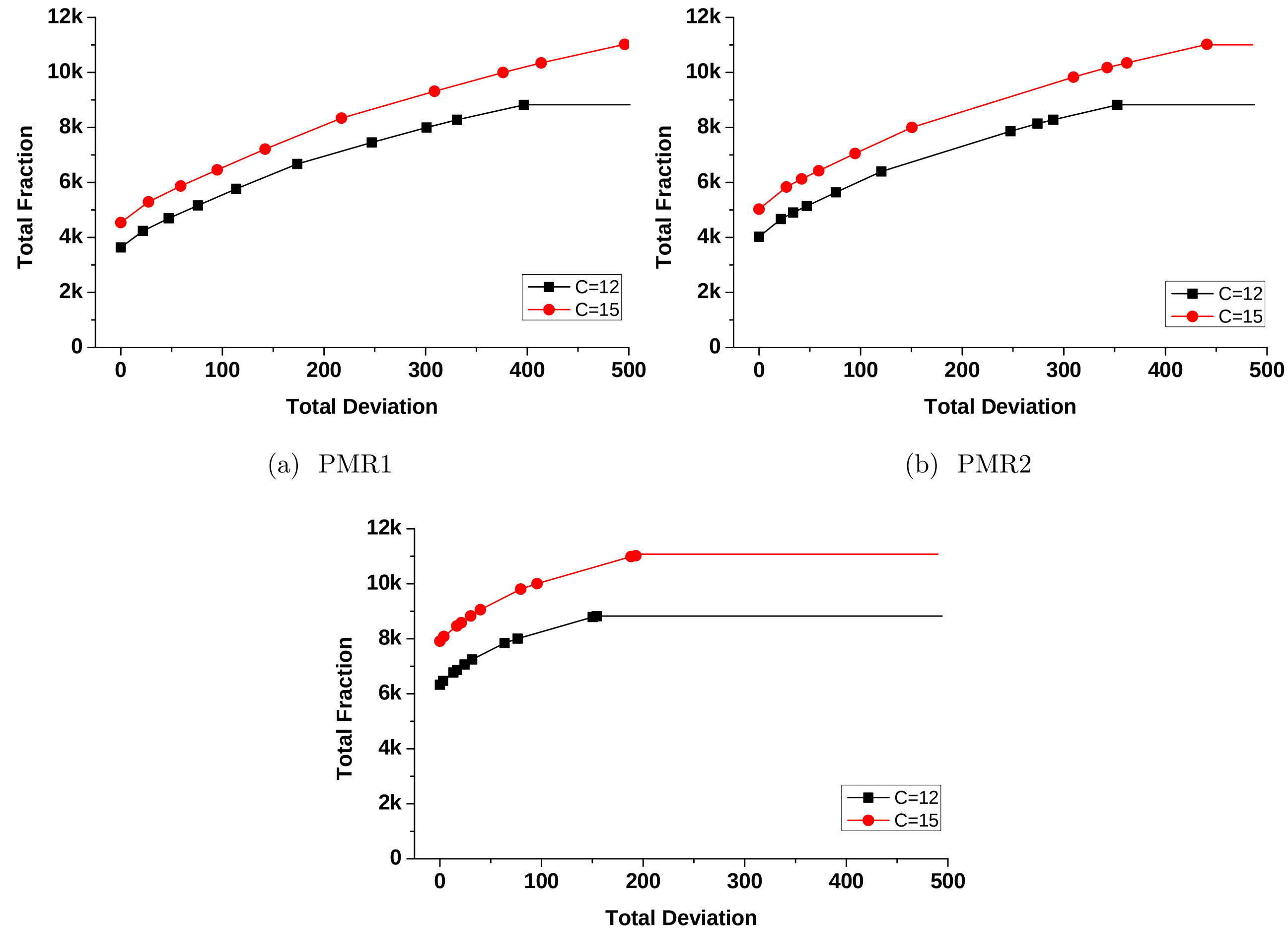

(a) PMR1

(b) PMR2

(c) PMR3

Figure 14: Impacts of C on BID frontiers

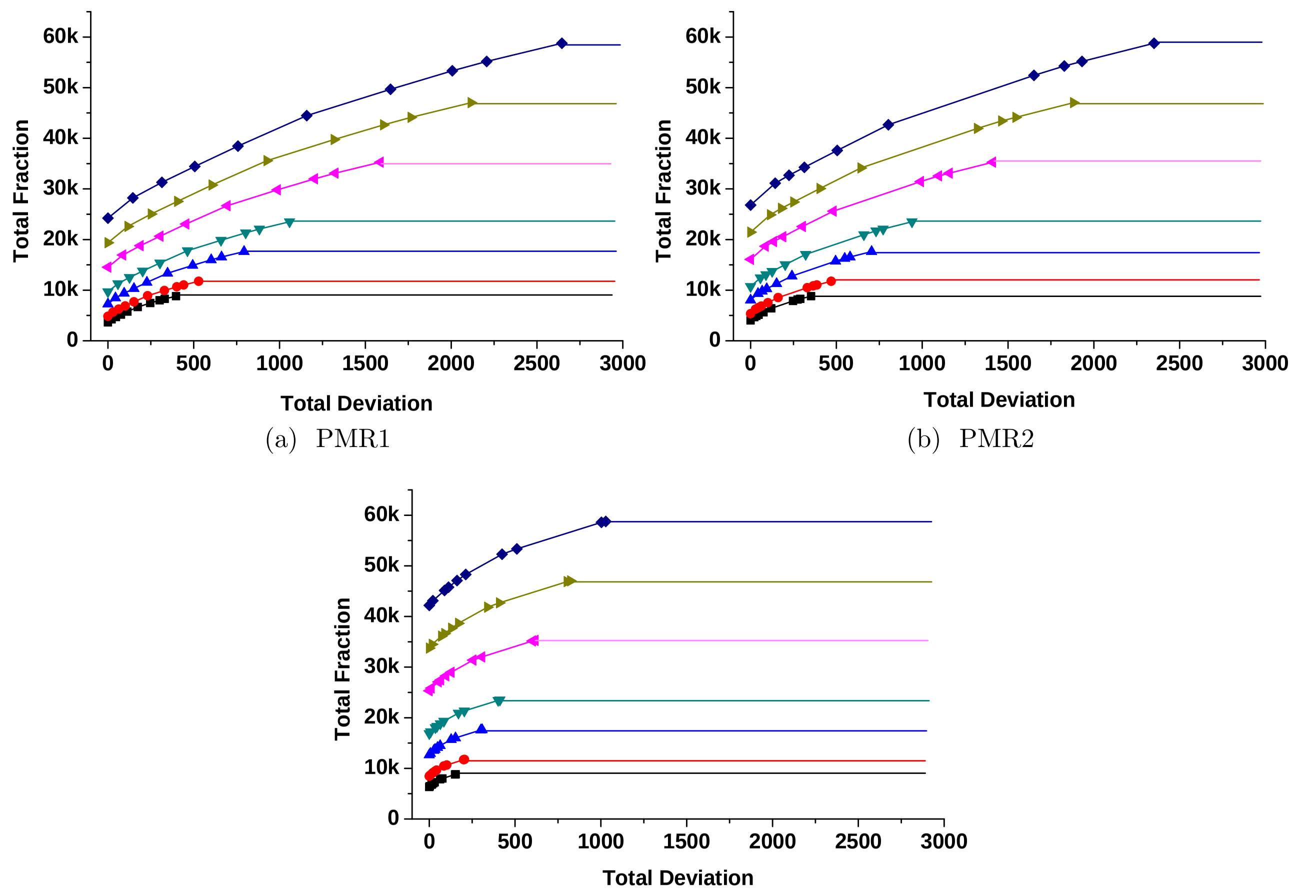

(a) PMR1

(b) PMR2

(c) PMR3

Figure 15: Impacts of T on base model frontiers

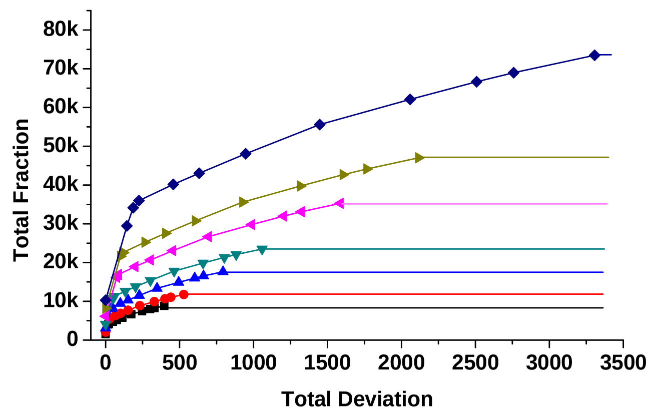

(a) PMR1

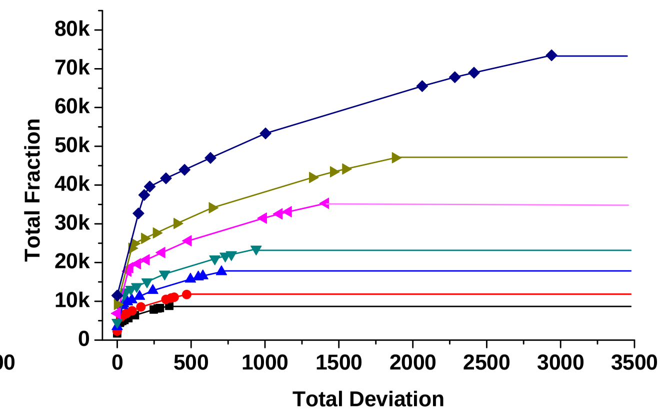

(b) PMR2

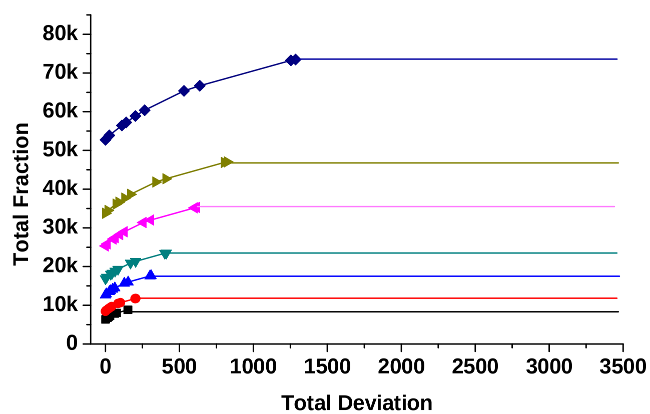

(c) PMR3

Figure 16: Impacts of T on anesthesia frontiers

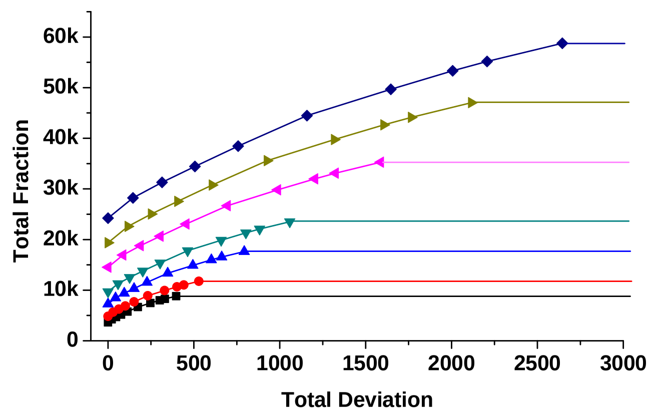

(a) PMR1

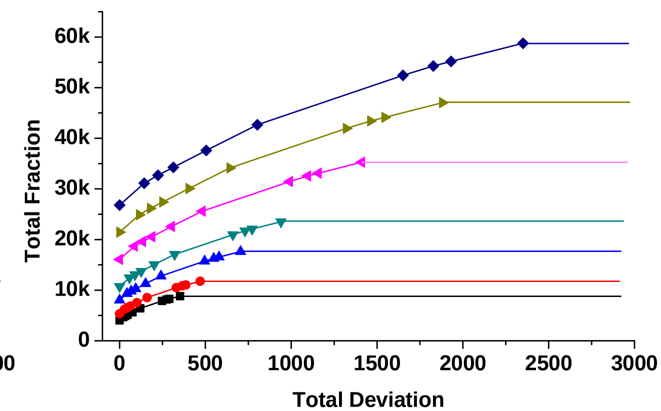

(b) PMR2

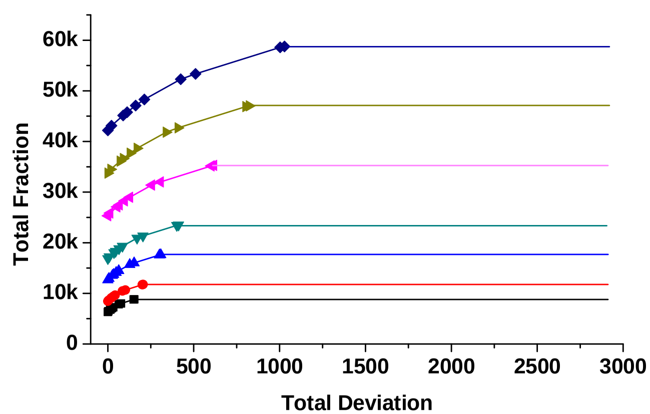

(c) PMR3

Figure 17: Impacts of T on BID frontiers ($\tau = 6$ hrs)

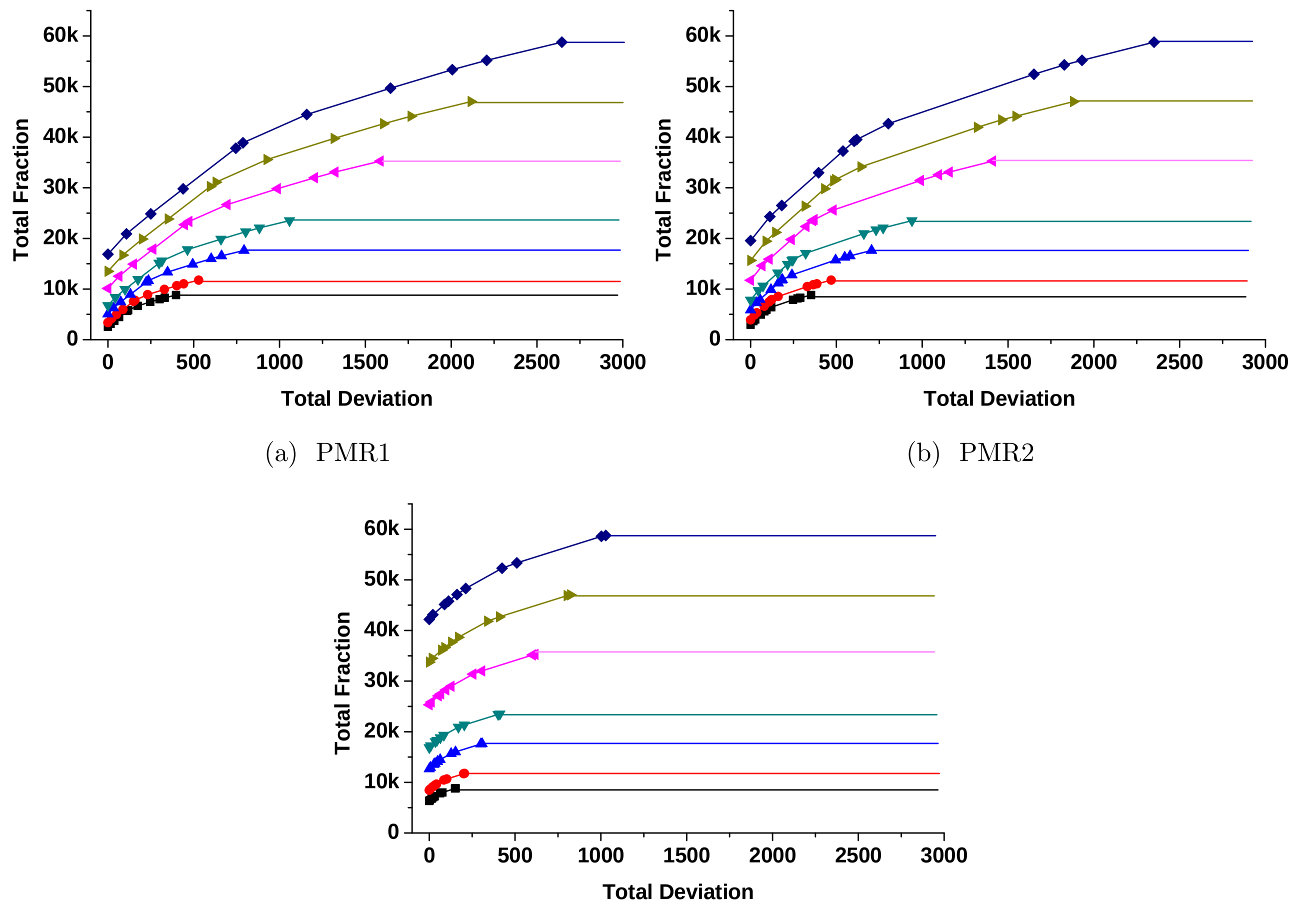

(a) PMR1 (b) PMR2

(c) PMR3

Figure 18: Impacts of T on gantry specializing frontiers

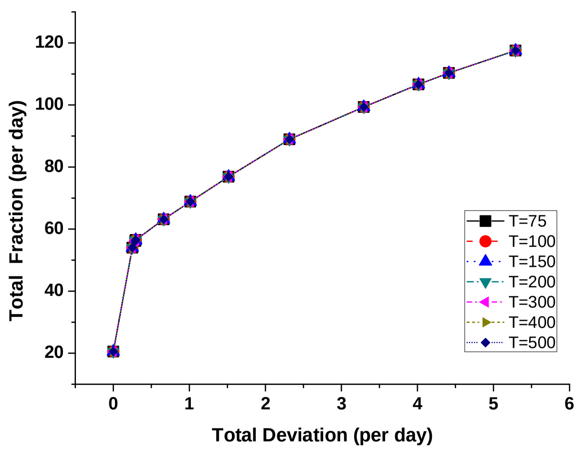

(a) PMR1

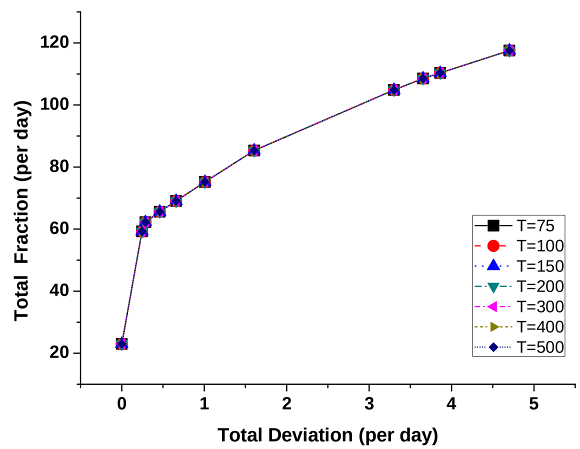

(b) PMR2

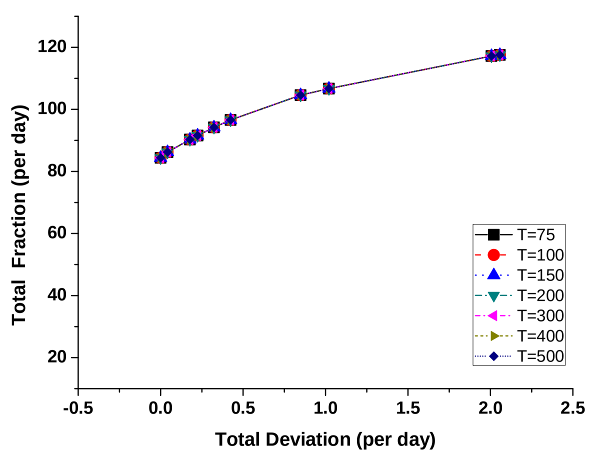

(c) PMR3

Figure 19: Normalized T anesthesia frontiers , $T \geq 75$

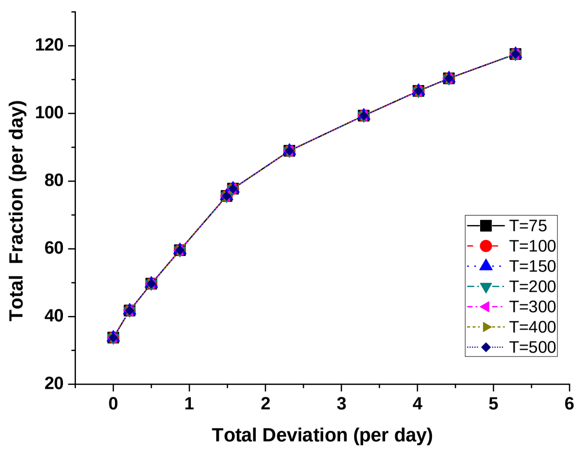

(a) PMR1

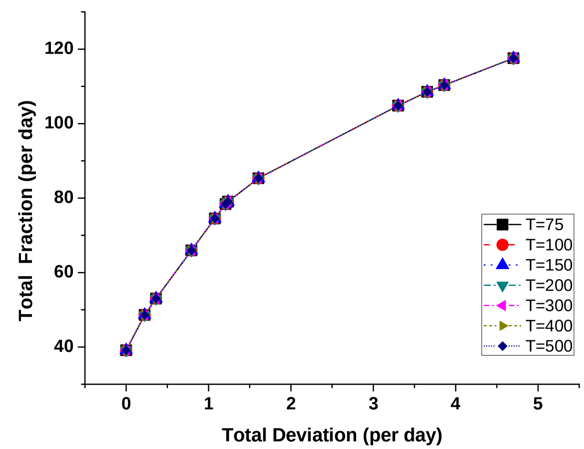

(b) PMR2

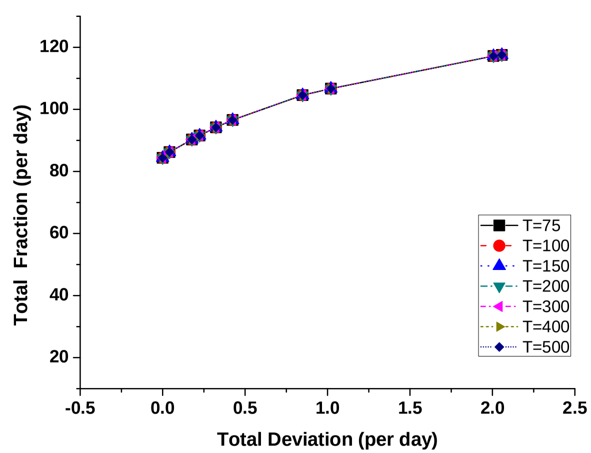

(c) PMR3

Figure 20: Normalized T gantry specialization frontiers , $T \geq 75$

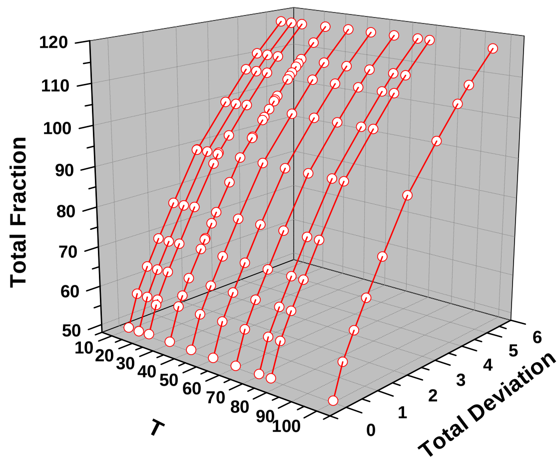

(a) PMR1

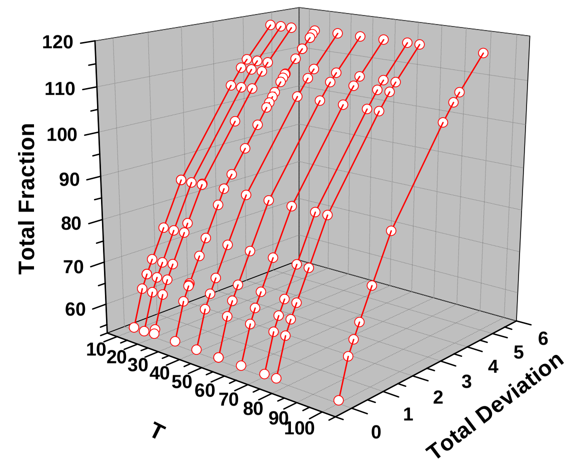

(b) PMR2

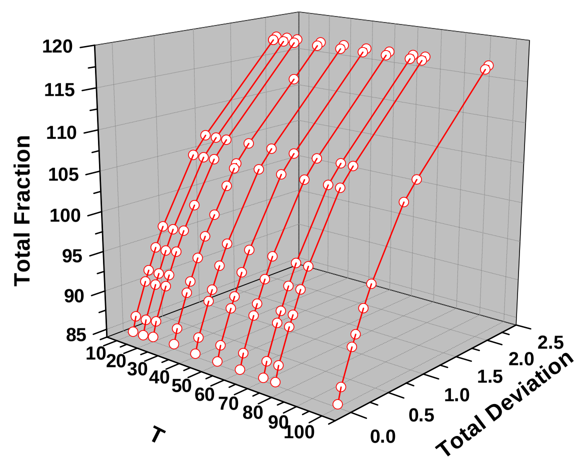

(c) PMR3

Figure 21: Three dimensional normalized T base model frontiers

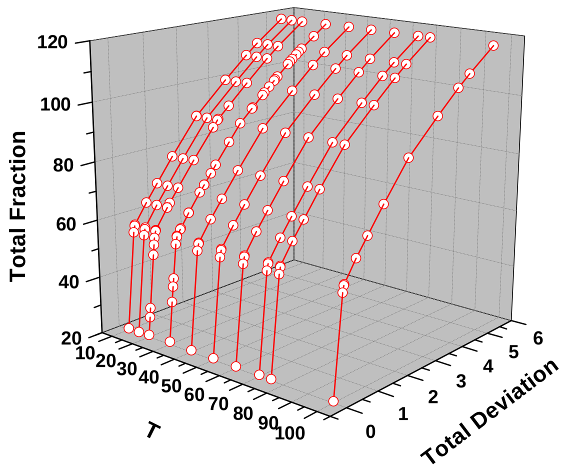

(a) PMR1

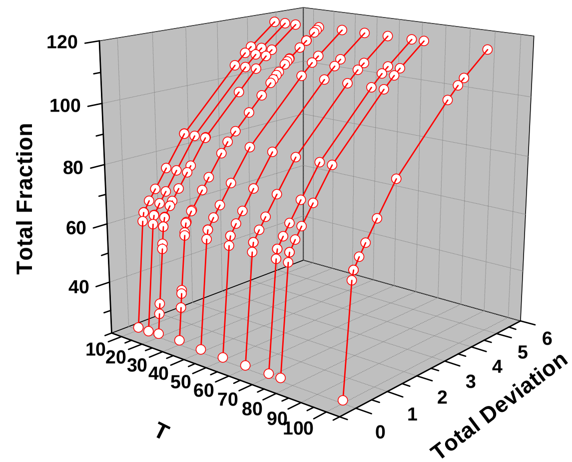

(b) PMR2

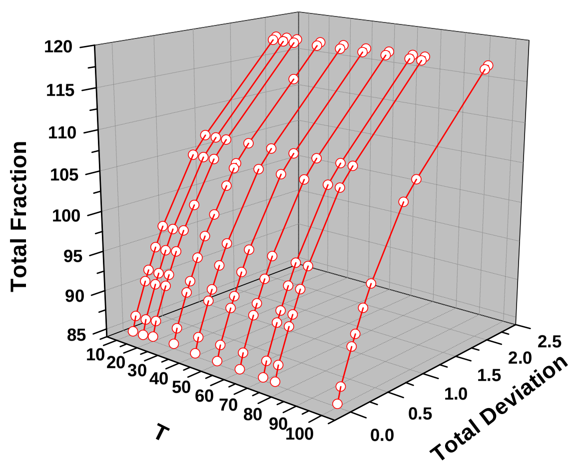

(c) PMR3

Figure 22: Three dimensional normalized T anesthesia frontiers

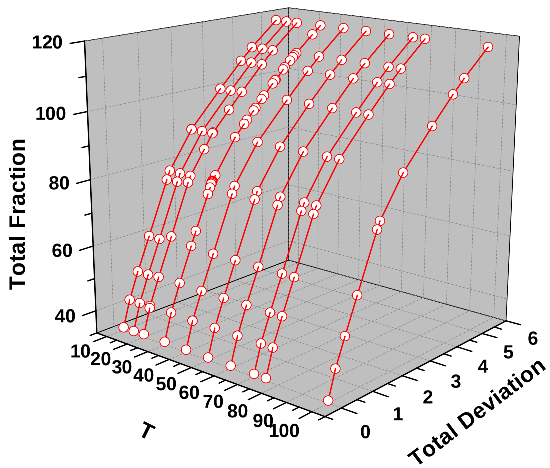

(a) PMR1

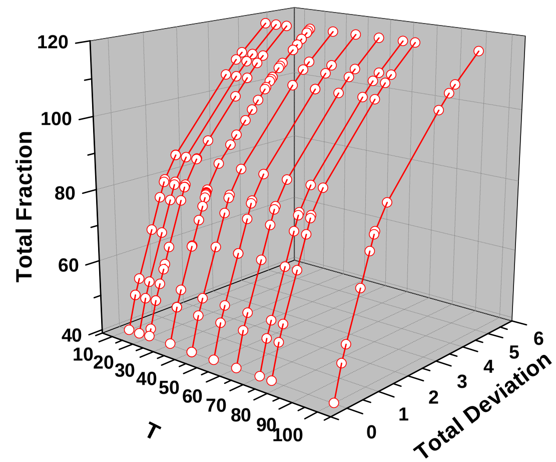

(b) PMR2

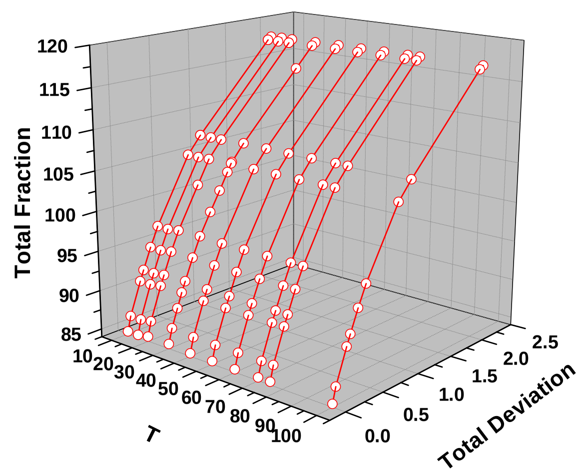

(c) PMR3

Figure 23: Three dimensional normalized T gantry specialization frontiers